

Margot SMITH

Nanotech for ICTs

2019

Laboratory for Soft Bioelectronic Interfaces

Implementation of medical grade material in Soft Neural Implants for Clinical Use

from 25/02/19 to 27/08/19

Confidentiality : yes

Under the supervision of :

- **Company supervisor : Nicolas VACHICOURAS, nicolas.vachicouras@epfl.ch**
Present at the defense : yes
- **Phelma Tutor : Youla, MORFOULI, youla.morfouli@phelma.grenoble-inp.fr**

**Ecole nationale
supérieure de physique,
électronique, matériaux**

Phelma
Bât. Grenoble INP - Minatec
3 Parvis Louis Néel - CS 50257
F-38016 Grenoble Cedex 01

Tél +33 (0)4 56 52 91 00
Fax +33 (0)4 56 52 91 03

<http://phelma.grenoble-inp.fr>

Abstract :

In the context of implantable subdural electrodes, the project aims to facilitate the translation towards clinical use of a new type of neural implants, SOFT ElectroCorticoGraphic (ECoG) electrodes. These soft subdural electrodes present the advantage of being more compliant and less damaging to neural tissue than most of the previous models.

The main focus of this project is the silicone material, the substrate of the device, and its interaction with gold layers, which form the interconnects and electrodes and that allow the devices to be stretchable and still conductive after an elastic deformation, thanks to the formation of microcracks.

Through electromechanical characterization we tested multiple medical grade materials, and found that two biocompatible silicones, the Silbione® M130 from Elkem and the Nusil™ 4211, meet our expectations, such as electrical resistance stability over stretching cycles. Another aspect of the soft ECoG is its hermeticity towards body fluids. Thus experiments detailed in the report were dedicated to understanding the limits and effects of such body fluids on the bonding of silicone-silicone interfaces through T-peel tests. A final experiment, an adjacent tracks insulation verification on soaking samples, was very promising as samples didn't show signs of failure for a soaking period of 31 days.

Finally, to set the project in the context of the translation towards the clinic, one should be given the administrative and management elements that allow such translation. Hence, a part of this report is dedicated to the synthesis of such requirements, specific to medical grade devices regulation

Résumé :

Dans le contexte d'implants neuronaux placés sous la dure-mère, le projet a pour but de faciliter la transition vers une utilisation clinique d'un nouveau type d'implant, les électrodes SOFT ElectroCorticoGraphique. Ces électrodes sous-durales molles présentent l'avantage de mieux se conformer à la surface complexe du cerveau, ainsi que d'engendrer moins de dommages sur le tissu neuronal que leurs prédécesseurs.

Le matériau qui est au centre de cette étude est le silicone ainsi que son interaction avec une couche d'or qui, grâce à la formation de micro-craquelures, permet au système d'être étirable et de rester conducteur après avoir été étiré. A travers une caractérisation électromécanique plusieurs matériaux biocompatibles ont été testés, dont deux ont été retenus pour une prochaine implémentation sur le système, du fait de la stabilité de la résistance électrique après plusieurs cycles d'étirement, le Silbione® M130 d'Elkem ainsi que le MED-4211 de Nusil™. Un autre aspect traité durant ce projet est l'herméticité de l'encapsulation des pistes d'or vis-à-vis des fluides corporels. Cette herméticité est rendue possible par une adhésion réalisée par oxydation de la surface du silicone par un plasma à oxygen. Ainsi des éprouvettes ont été testées pendant une immersion en solution PBS durant 31 jours, ce qui a permis de montrer l'absence de courts-circuits tout au long de cette période.

Sommario :

Nel contesto degli elettrodi impiantabili subdurali, questo progetto mira a favorire il passaggio da laboratorio a uso clinico di un nuovo tipo di dispositivi, gli elettrodi per ElelettroCorticoGrafia (ECoG) morbidi. Questi morbidi elettrodi subdurali presentano il vantaggio di essere più conformabili e meno dannosi per i tessuti, rispetto a modelli sviluppati in passato. Al centro di questo progetto vi è lo studio del silicone, il substrato del dispositivo, e della sua interazione con gli strati di oro che formano gli elettrodi e le connessioni e che permettono ai dispositivi di estendersi e mantenere al contempo la conduttività anche a seguito di deformazione, grazie alla formazione di microfratture.

Attraverso esperimenti di caratterizzazione elettromeccanica è stato possibile testare diversi materiali biocompatibili approvati per uso medico e individuarne due, il Silbione® M130 prodotto da Elkem e il Nusil™ 4211, che soddisfanno i requisiti necessari in termini di stabilità della resistenza elettrica a seguito di deformazioni cicliche. Un altro aspetto rilevante degli ECoG è l'ermeticità rispetto ai liquidi corporei. Sono perciò presentati in questo lavoro esperimenti dedicati alla comprensione dei limiti e degli effetti di tali liquidi sull'adesione all'interfaccia silicone-silicone, come le prove di peel a T. Un esperimento finale sulla verifica di cortocircuito su campioni soggetti a immersione ha permesso di ottenere risultati promettenti, in quanto non sono stati rilevati segni di fallimento per 31 giorni.

Per concludere, al fine di inquadrare il progetto nel contesto di un passaggio alla clinica, è necessario fornire un resoconto degli elementi amministrativi e gestionali che permettono tale passaggio. Per questo motivo una parte di questa tesi è dedicata alla sintesi dei requisiti specifici previsti dalle normative per dispositivi medici.

CONTENT

1	Introduction	6
1.1	Brain surgery and monitoring.....	6
1.2	Clinical subdural electrodes	7
1.3	New generation of subdural electrodes	8
1.4	Project's objectives	9
2	Transition to medical grade material	10
2.1	Current technology.....	10
2.2	Theory	11
2.2.1	Microcracked Gold.....	11
2.2.2	Silicone and plasma bonding	13
2.3	Materials and Method.....	18
2.3.1	Types of silicones	18
2.3.2	Fabrication of silicone	18
2.3.3	Bonding test.....	18
2.3.4	Stiff backing	20
2.3.5	Aging tests	21
2.3.6	Electromechanical characterization	22
2.4	Results and Discussion	24
2.4.1	Bonding tests	24
2.4.2	Aging process.....	26
2.4.3	Electromechanical characterization	29
2.5	Conclusion	30
3	Design of protocols for systematic development	31
3.1	Regulatory requirements	31
3.1.1	Biocompatibility.....	32
3.1.2	Other soft ECoG clinical translation.....	32
3.1.3	Administrative procedure.....	32
3.2	Adjacent tracks electrical insulation.....	35
3.2.1	Materials and method	35
3.2.2	Results and discussion	36
4	Conclusion.....	39
5	Future prospects	40
6	Références.....	41
7	Annexes.....	43

LIST OF FIGURES

Figure 1 : Example of subdural electrodes implanted on a patient's brain to identify epileptic foci.....	6
Figure 2 : Schematic of multiple technologies with a)Neural signals, b)Position of the implants and c)Description of devices and signals [1].....	7
Figure 3 : Structure of conventional stiff clinical subdural electrodes currently on the market	8
Figure 4 : Comparison of a contemporary clinical subdural electrode (left) on the surface of a brain mold compared to a Soft ECoG (right).....	8
Figure 5 : Soft strip of Wise neuro (left) and Soft ECoG grid of the LSBI (right) (property of LSBI).....	9
Figure 6 : Exploded view of a SOFT ECoG, gold tracks are sandwich between two silicone layers to create an encapsulation; SEM image of microcracks (bottom left) and SEM image of composite electrode (bottom right) (property of the LSBI)	10
Figure 7 : Microcracks formation through history [7] [6] [9].....	12
Figure 8 : Schematic of an elongation cycle of the gold tracks.....	12
Figure 9 : Examples of resistance evolution throughout the years [7] [13] [14]	13
Figure 10 : Data on silicones comparison, M. Roulet(property of LSBI)	14
Figure 11 : Multiple examples of previous improvement on materials, J. Bourely [18] (property of LSBI)	15
Figure 12 : Plasma bonding schematic	15
Figure 13 : Bonding strength tests examples [21] [23].....	16
Figure 14 : Peeling test model, Eitner et al.....	17
Figure 15 : Plasma bonding steps (a)Surface activation through plasma (b-c)Flipping one slice to go on top of the other, with a PET sheet to protect half of the slice to bond and (d)the final bonded sample .	18
Figure 16 : T-peel experiment for bonding test schematic (a-1)Dimensions of silicones samples (a-2) T-peel test positioning of the samples (b) Stacks installed in clamps and (c)Picture of installed samples .	19
Figure 17 : Typical output to expect during a bonding test of peeling force on the elongation, the blue curve indicate a cohesive failure, while the red curve indicate an adhesive failure.....	20
Figure 18 : Schematic of the fabrication of stiff backing samples, in (a)the oxygen plasma activation of the surface, then (b.1-2)use of PET sheet fixed with RTV and (c)tape (Kapton) application	21
Figure 19 : Accelerated aging sample example, soaking up until 4 months, at 2 temperatures	21
Figure 20 : (a)Example of sample to be stretched and (b)example of arrangement of samples and strips on the wafer	22
Figure 21 : Sheet resistance measurement set-up	23
Figure 22 : Electromechanical characterization schematics and pictures; (a) Sample to be stretched (x) composed of 8 gold tracks (n) (b) Set-up (main pieces)	23
Figure 23 : Bonding test of Sylgard 184© samples (purple, n=4) and Silbione® M140 1day after plasma (pink,n=3)	24
Figure 24 : Stiff-backing T-peel test.....	25
Figure 25 : Stiff-backing bonding tests of Silbione® M140, with PET bonded with plasma (yellow, n=2), PET fixed with RTV (blue, n=3) and adhesive tape (purple, n=1).....	26
Figure 26 : Bonding test on Silbione® M140 1day after plasma (pink, n=3), 1week after plasma in PBS solution at 37°C (blue, n=4), 2 weeks after plasma in PBS solution at 37°C (green, n=3) and 4 months after plasma (clear-blue, n=3)	27
Figure 27 : Accelerated aging test following Arrhenius law [24]	28
Figure 28 : Normalized resistances of all materials (avg+std on n tracks), Sylgard 184 (blue), Silbione® M130 (orange), Silbione® M140 (yellow), Nusil™ 4211 (purple) and Nusil™ 4210 (green) through electromechanical characterization; each material except for the Silbione®M130 has a gold layer of 35nm	29

Figure 29 : Roadmap of a clinical device [27] adapted from [28], property of the LSBI	31
Figure 30 : Adapted from R. K. Shepherd [30], Application of Design Controls to Design process.....	33
Figure 31 : Administrative forms trough which an operator has to conduct its experiment for an experiment as part of the Design output	33
Figure 32 : Electrical insulation hermeticity experiment set-up.....	35
Figure 33 : Adjacent tracks current leakage tests on Silbione® M140 show an evolution of the inter- channel resistance through time.....	36
Figure 34 : Adjacent tracks current leakage tests on Sylgard 184© show an evolution of the inter- channel resistance through time.....	37
Figure 35 : Normalized impedance (avg+std) of the stretched samples after 31 days soaking in a PBS solution at 37°C, Sylgard 184© (blue, n=3) and Silbione® M140 (dark orange, n=1).....	37
Figure 36 : Silbione M140 stretching cycles all seperated.....	45
Figure 37 : Nusil™ MED-4211 stretching cycles all seperated	45
Figure 38 : Nusil™ MED-4210 stretching cycles all seperated	45
Figure 39 : Silbione® M130 stretching cycles all seperated.....	46

LABORATORY FOR SOFT BIOELECTRONIC INTERFACES

The LSBI is a multidisciplinary group at the cross roads of biology and engineering. The research conducted there explore materials, technologies and integration of soft bioelectronic interfaces or electronic skins. There, stretchable materials and devices are designed and characterized towards their implementation in ultra-compliant circuitry, soft biointerfaces, and are reaching out to a potential translation to the clinic. The files of applications of Soft BioElectronic interfaces is very broad, from state-of-the-art user touch interfaces to long-term active neuroprosthesis.

ACKNOWLEDGEMENT

I first would like to thank Stéphanie Lacour for giving me the opportunity to work on this project in the Laboratory for Soft Bioelectronic Interfaces, as it has been a great human and academic experience.

I would like to thank my supervisors team as well, Nicolas Vachicouras for having me on the project but also for his guidance along the project and on this thesis, Ludovic Serex for his assistance in the lab and his motivation for the sport sessions, and Florian Fallegger for the time he spent teaching me every manufacturing steps.

I also want to thank the whole team of the LSBI for their guidance and the laughs.

I wouldn't have been able to do this Master Degree without the whole team of professors and the administration that are behind the Nanotech program, from the three host institutions.

Finally I would like to thank my family and my friends, as they have always been supporting in many ways, anytime, and without whom none of this would have been possible.

1 INTRODUCTION

1.1 BRAIN SURGERY AND MONITORING

Increasing number of people are in need of brain surgery. One common intervention on the brain is the removal of a tumor present in the brain. One of the risks associated with brain tumor removal is the removal or deterioration of functional brain regions that could impair even more the patient afterward. Therefore surgeons use electrodes during surgery to constantly map the brain and assure themselves that they are not damaging important part of the cortex. The mapping can be done by combining both recording and stimulation, as shown on Figure 1. Another intervention is the removal of the brain region that causes the epileptic seizures (known as “epileptic foci”) in people suffering from drug resistant epilepsy. There, before the surgical intervention the neurologist has to determine the position of said foci, and even if it can partially be done through functional Magnetic Resonance imaging (MRI) or with an EEG, subdural electrodes are also used as more precise. During a pre-surgical phase the subdural electrodes are implanted to localize the foci to be removed. The size of the grid that will cover the surface of the brain (and determine the location) depends on how well the neurologist has been able to localize the targeted region with non-invasive technics (MRI, EEG), typically the subdural grid/strip covers a very broad region of the brain.



Figure 1 : Example of subdural electrodes implanted on a patient's brain to identify epileptic foci

After surgery, while the patient stays at the hospital, the electrodes are connected to neuromonitoring system that constantly records the brain activity. This waiting periods aims to wait for an epileptic seizure to happen, during which the brain signals will be recorded and then analyzed by the neurologist to determine the region of the foci. The patient then undergoes a second surgery during which the epileptic foci is removed, while the intraoperative neuromonitoring can still be used to avoid removal of the eloquent cortex.

The tools used to help surgeons, either for mapping or for monitoring of the brain are called neural implants and can be found in multiple shapes or form depending on the need of the situation. They often consist of an array of electrodes that aim to restore impaired functions of the nervous system through electrical stimulation and/or recording of the neural tissue. Some of these neural implants are meant to be used as interfaces with the brain and serve multiple clinical purposes. For example these electrodes can be used as epilepsy monitoring unit for the localization of a seizure [1], or create a brain-machine interface (or Brain-Computer Interfaces, BCI) with a tetraplegic patient [2]. There are various strategies for the electrodes to interface with the brain to stimulate or record neural activity. These can be grouped in three main types of electrodes according to their invasiveness :

- **ElectroEncephaloGraphy (EEG)** electrodes are non-invasive electrodes positioned around the head similarly as a helmet to record broad neural activity
- **ElectroCorticoGraphy (ECoG)** are surgically implanted/positioned electrodes on the surface of the brain, below the dura (protective skin of the brain surface) and allow a more accurate recording
- Penetrating **MultiElectrodeArrays (MEAs)** are highly invasive devices that penetrate the brain and allow a much more precise recording of single neuron activity.

These multiple strategies are summarized in Figure 2. ECoGs, also known as subdural electrodes, appear as a good trade-off as a less invasive strategy than penetrating MEAs, yet with a closer contact to the tissue, allowing a more precise recording and/or stimulation of neurons, compared to EEG.

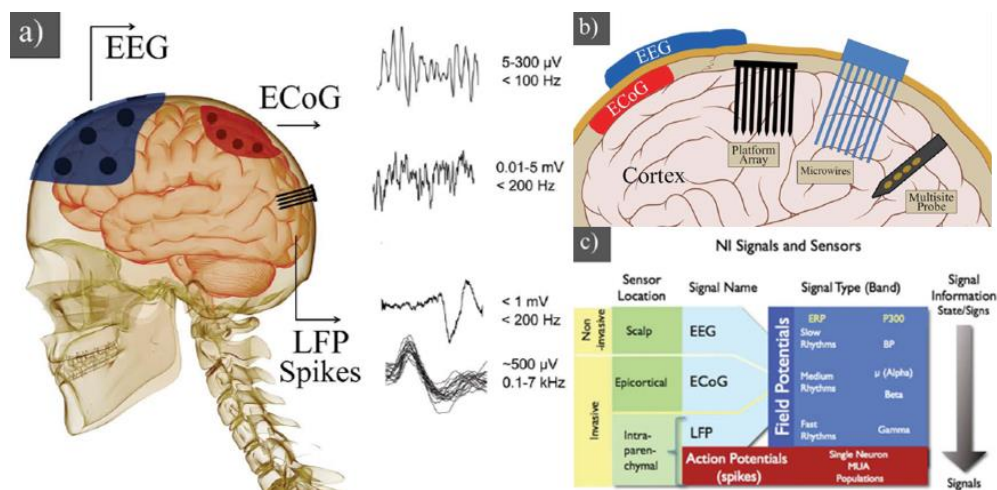


Figure 2 : Schematic of multiple technologies with a) Neural signals, b) Position of the implants and c) Description of devices and signals [1]

Subdural electrodes have two types of clinical uses :

- Mapping of functional brain regions before a brain surgery, known as **intraoperative neuromonitoring** (use less than 24hours)
- Detection before surgery of drug-resistant epilepsy cases, known as **pre-surgical epilepsy detection** (use less than 30 days)

1.2 CLINICAL SUBDURAL ELECTRODES

Today subdural electrodes are manufactured and sold by three main companies : Ad-Tech®, Dixi medical© and PMT® corporation. These clinical grids are however 1 to 3 millimeter in thickness, stiff and thick platinum disk are embedded to serve as electrode contact, further increasing the stiffness of the electrode. These mechanical characteristics are not optimal for brain interfacing as they don't conform the complex structure of the brain's curvature, which lead to have some electrodes unable to be in

contact with the tissue. Their stiffness might increase the risks of hematomas. Similarly their electrodes are rather large and bulky, leading not only to a limitation of the precision on the covered surface but also to induce more damage to the tissue (dimensions of such subdural electrode's side view on Figure 3).

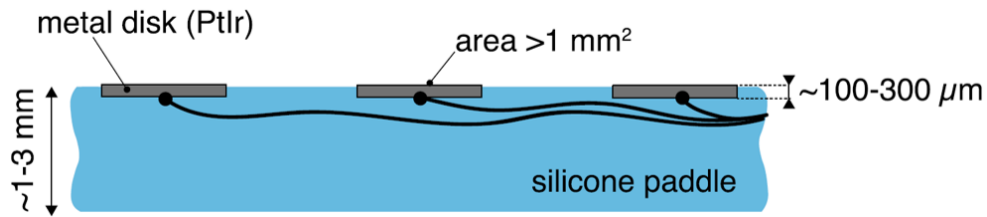


Figure 3 : Structure of conventional stiff clinical subdural electrodes currently on the market

These multiple issues encouraged the development of thinner, more conformable subdural bioelectronic devices.

1.3 NEW GENERATION OF SUBDURAL ELECTRODES

The Soft ECoG developed at the LSBI uses a much softer (elastic modulus of 1Mpa) and thinner ($400\mu\text{m}$) silicone substrate, allowing the subdural electrode to be more conformable to the complex brain structure and allows a better contact (see on Figure 4). Here the electrodes and electrical wires are replaced by elastic coating and stretchable conductors to improve the overall device softness. Furthermore those devices could decrease risks of hematomas for a denser and higher amount of electrodes.



Figure 4 : Comparison of a contemporary clinical subdural electrode (left) on the surface of a brain mold compared to a Soft ECoG (right)

These technologies seem promising, but bringing them to the clinic require a lot of work. Because they use unconventional materials one would need to demonstrate the safety, reliability and conformability to regulation requirements of such materials. As of today, no soft ECoGs are yet approved for commercialization, however Wise (see Figure 5) and the LSBI are taking the path towards first clinical trials and going through the medical regulation pathway to bring these devices to the clinic.



Figure 5 : Soft strip of Wise neuro (left) and Soft ECoG grid of the LSBI (right) (property of LSBI)

The first step towards the translation of these technologies to the clinic is the transfer from research grade materials to medical grade materials (Obidin et al. [3]).

1.4 PROJECT'S OBJECTIVES

The main objective of my project is to assist the translation toward this change of materials by identifying the needs and specifications of a SOFT ECoG, setting test bench and methodologies to screen and select adequate medical grade materials, to replace the current research grade materials by medical grade ones.

One great endeavor in implantable devices is hermeticity to liquid and ions. The hermetic encapsulation allows to protect the patients by avoiding the loss of material (such as chromium that can be toxic), but also prevent inter-channel crosstalk that could jeopardize the neural recording and/or stimulation. Thus by changing material it is of utmost importance to insure this hermeticity especially at the interface between layers or materials. The tests conducted during this project aim to understand the limits of the encapsulation in environment mimicking *in-vivo* conditions. This aspect has mainly been tackled through bonding test.

Furthermore, the relation between gold and silicone is a key parameter for the SOFT ECoG, and it is an important factor in the choice of medical grade silicone. Electromechanical characterization tests were performed on fully developed samples to analyze the behavior of microcracked gold through stretching.

Finally the translation to clinic require adaptation of the documentation of experiment as well, therefore an overview of the requirements from the regulation organisms is presented.

2 TRANSITION TO MEDICAL GRADE MATERIAL

2.1 CURRENT TECHNOLOGY

The novelty of the Soft ECoG is primarily in its use of soft materials and new manufacturing processes compared to current clinical subdural electrodes.

At the LSBI we have been able to manufacture electrode arrays that are soft and reversibly stretchable, meaning that their electrical performance remains functional. This is possible thanks to a unique technology that allows the patterning of thin gold tracks (<50nm in thickness) on a silicone substrate (of $100\mu\text{m} - 400\mu\text{m}$ thick) that contains microcracks (as shown on bottom left of Figure 6). These microcracks allow the gold track to elastically deform while maintaining a percolating pathway for the current to go through, thus allowing the track to remain conductive even under stretching conditions. Moreover the electrodes sites are coated with a platinum-silicone stretchable composite that allow conformability and a low impedance interfaces with the neural tissue. Further details on the fabrication process are given in annexes.

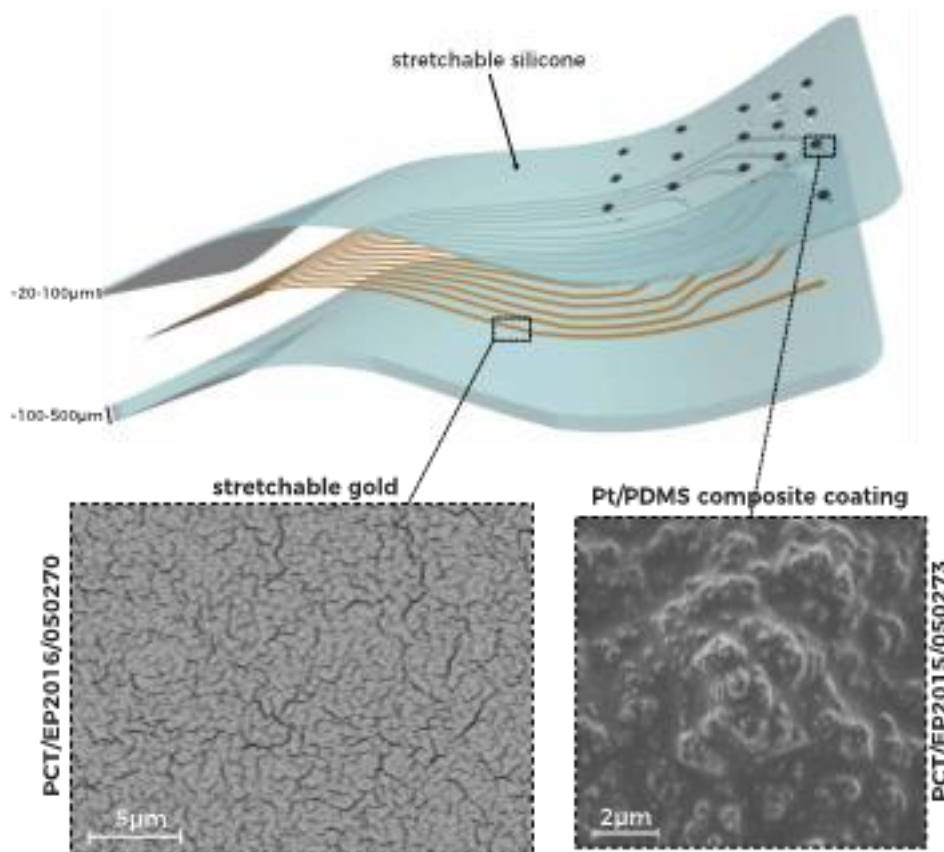


Figure 6 : Exploded view of a SOFT ECoG,
gold tracks are sandwich between two silicone layers to create an encapsulation;
SEM image of microcracks (bottom left) and SEM image of composite electrode (bottom right) (property of the LSBI)

As highlighted by Obidin et al. (2019) [3] one way to facilitate the transition to medical grade technology is to use biocompatible, thus already approved material. The silicone encapsulation was identified as the most critical component of the device. Indeed the silicone is the material that has most of its surface in contact with the tissue, and its physical characteristics impacts various functionalities of the device.

Moreover, another important aspect is that the silicone substrate impacts the formation of microcracks in the gold layer. These microcracks are an important feature as they enable the gold to conduct electricity even after the device has been stretched several times. Moreover the parameters that are at the origin of their formation are numerous (as listed by Graudejus et al., 2010 [4]), and not always easily controllable.

Understanding the formation of the microcracks is of great importance if one wants to change the silicone on which the gold is deposited. The following chapter will focus on the theory behind the formation of such microcracks and will provide insight on the bonding of such material in order to make an informed choice on the medical grade silicone meant to replace the laboratory grade one in the path toward clinically approved devices.

2.2 THEORY

2.2.1 Microcracked Gold

Gold is an interesting material for soft bioelectronic applications due to its good conductivity ($\sim 4.10 \times 10^7 \frac{S}{m}$, [5]) and for its biocompatibility [6] [5]. Moreover, compared to silver or copper, it has a better chemical stability, making it less subject to oxidation and corrosion in ambient conditions [5]. Unfortunately, like most metals, the mechanical properties of gold are not compatible with soft stretchable electrodes, as it shows a ductile behavior and will deform plastically for a very low applied strain, until complete failure. Nevertheless Lacour et al. (2003, 2006) showed that, under certain fabrication conditions, thin films ($\sim 35\text{nm}$) of gold (for a $\sim 5\text{nm}$ adhesive layer of chromium or titanium) evaporated on poly(dimethyl)siloxane (PDMS)(Sylgard 184©) formed a microcracked structure [7] [6] [8] [5]. When stretching the silicone/gold construct, the gold around the microcracks can deflect out of plan, thus relieving the local strain while maintaining a percolating path for the current to go through (Lacour et al., 2006). Therefore this microcracked gold form a stretchable conductor. One of the challenge of microcracked gold is that these microcracks form under certain deposition conditions and only some silicone substrate. It is thus critical to understand well the mechanism of the formation of microcracks for the development of repeatable medical grade silicone/gold structures.

The first established review on which microcracked gold appear is the publication of Neves et al. (1999, [9]) in which different observation and measurement tools are compared such as AFM (Atomic Force Microscope), SPM (Scanning Probe Microscope) and FE-SEM (Field Emission Scanning Electron Microscope). To observe those microcracks, an Au film is sputtered on an epoxy resin block that was beforehand polished with diamond paste, forming a layer of $W = 17 \pm 3\text{nm}$ thickness of Gold. From the images of the paper there is a formation of said microcracks of the order of hundreds of nanometers depending on the crack (Figure 7-(a)).

In parallel Bowden et al. (1999) studied the evaporation of gold on elastomeric polymers such as PDMS (Poly(DiMethylSiloxane)), referred as silicone in the report) [10] [11] through e-beam PVD. It is however only from 2006 (Lacour et al.), that microcracks appear on elastomeric silicone under SEM observation (Figure 7-(b)(c)).

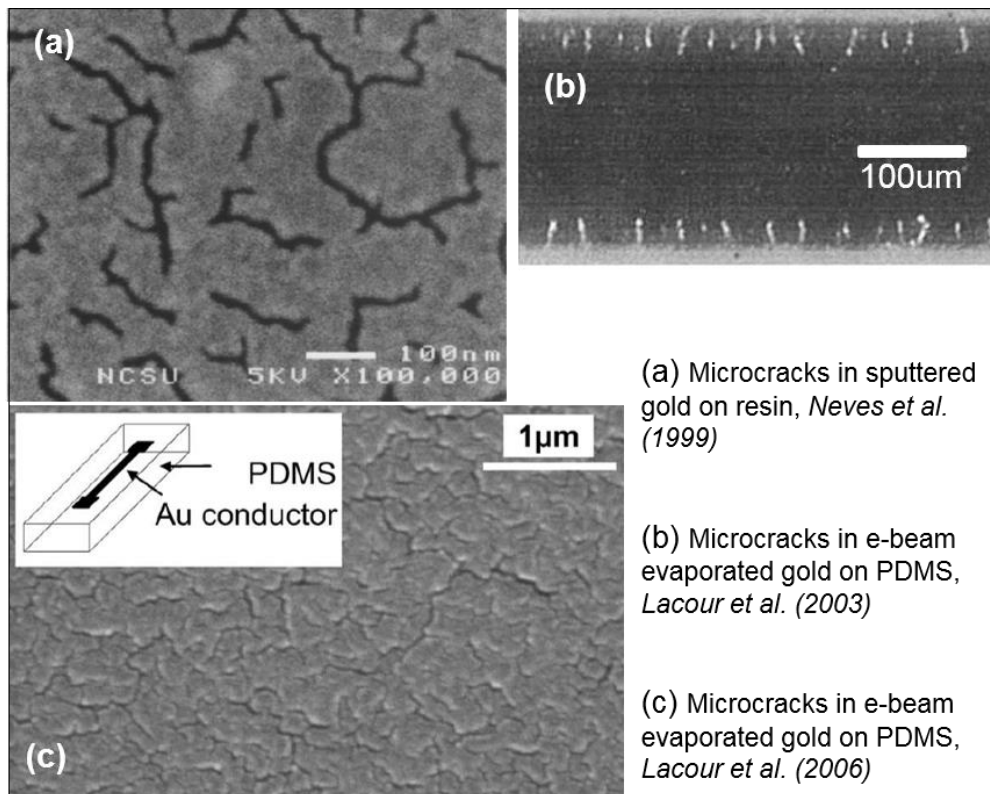


Figure 7 : Microcracks formation through history [7] [6] [9]

The formation of microcracks make it possible to obtain a flexible device, which mean that the device can still conduct while being stretched or after having been stretched. Graudejus et al. (2009, [12]) show that for an **uniaxial elongation of 30%** the SMEA keep conducting for more than 20 **cycles of stretching/relaxing**. Figure 8 shows a schematic of such cycle.

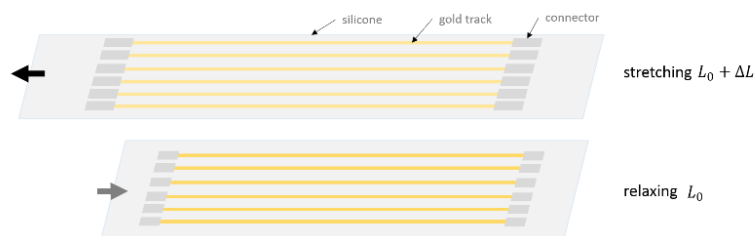


Figure 8 : Schematic of an elongation cycle of the gold tracks

Through the years and the improvement of the dimensions of the tracks, the deposition rate and the substrate, it is now possible to stretch through thousands of cycles, for 20 to 30% elongation, and still have a conducting device, as shown on Figure 9. (*Lacour et al., 2006 [7], Adrega et al., 2010 [13], Minev et al., 2015 [14]*).

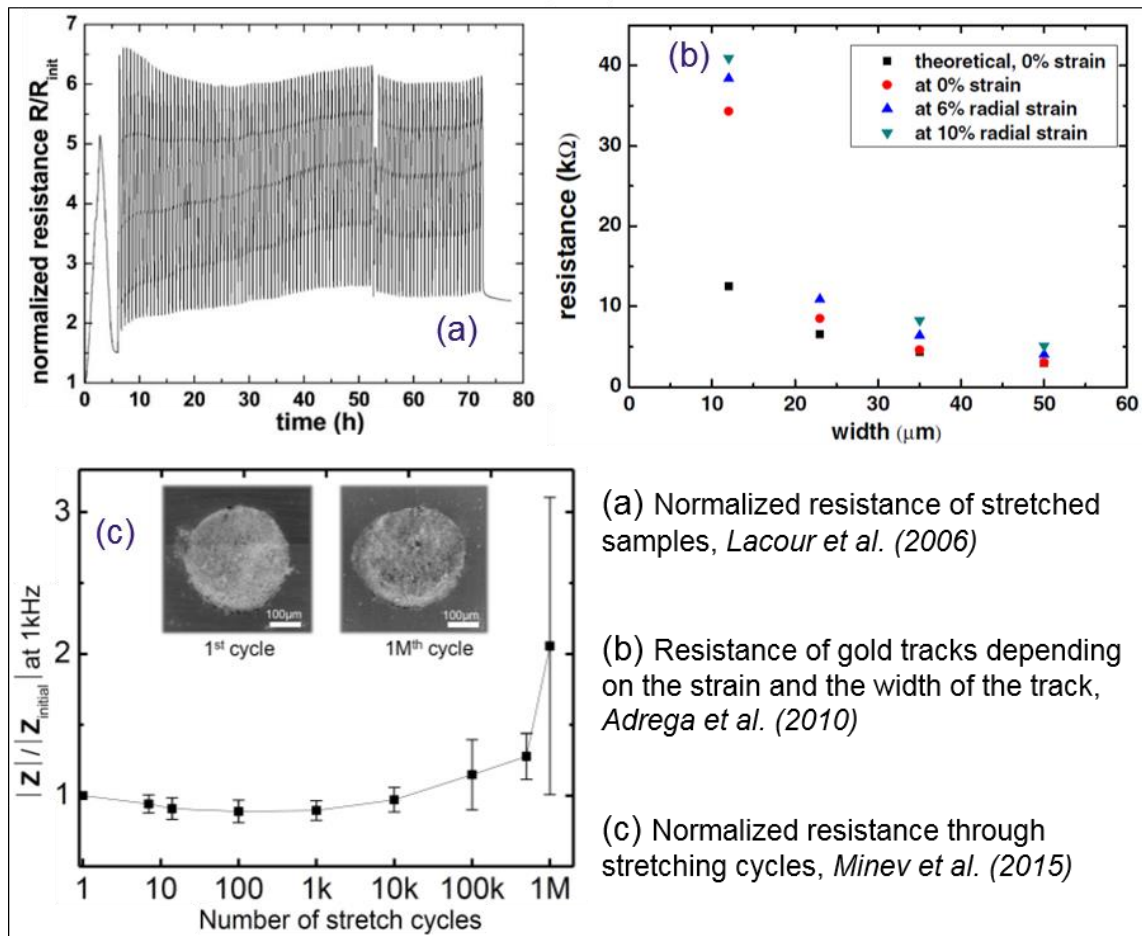


Figure 9 : Examples of resistance evolution throughout the years [7] [13] [14]

We refer to this cycle-through-stretching process as the electromechanical characterization. This test allows us to verify the proper functioning of a device, and to characterize the different materials and technics that are implemented around the device.

2.2.2 Silicone and plasma bonding

Another aspect that is tested in this project is the **hermeticity** of the device. In fact, as one can see on Figure 6, the gold tracks are sandwiched between two layers of silicone. The bonding of the silicone layers shall be hermetic to prevent any external elements to damage the gold tracks.

2.2.2.1 Aspects of silicone

PDMS is interesting for biomedical applications as it is non-toxic, visually clear but also thanks to its ease of fabrication and molding , and as its final form is a soft device and therefore doesn't trigger Foreign-Body Reaction (FBR, Minev et al. [14]). For its fabrication in most cases it comes as two parts that mixed together will lead to the cross-linking that will form the elastomeric polymer that is called silicone. In our case and similarly as Campbell et al. (1999) we use a kit of Sylgard 184 © from Dow Corning, in which the Part A is a pre-polymer of PDMS and a cross-linking agent and the Part B is an organometallic catalyst platinum-based. When the mix undergoes an annealing temperature a hydrosilation reaction allows the formation of silicone [15] . In the case of the Sylgard 184© the ratio between part A and part B is of 10:1, but other silicones preparations use a ratio of 1:1.

Silicones rubbers are classified mostly according to their viscosity and then their curing temperature. We can distinguish three main types of forms of silicones before the curing : Room Temperature Vulcanize

silicones (RTVs), Liquid Silicone Rubbers (LSR) and High Consistency Rubbers (HCR). HCR are more viscous and require the use of injected molds or extrusion for processing. On the other hand RTVs of LSR can be coated or poured in cast as more liquid. Those parameters are highlighted and more easily comparable in the Tableau 1.

Material	Curing temperature (°C)	Viscosity (cP)	Elongation (%)
Water	-	0.89	-
HCR	300 to 350	8'000 to 150'000	650 to 1000
LSR	110 to 200	2'000 to 100'000	350 to 550
RTVs	50 to 120	6'000	500

Tableau 1 : Characteristics of multiple silicones types before and after curing [16]

For the process and the application that is made of our devices, we choose materials for their biocompatibility, and if they allow the formation of microcracks. They are also chosen over mechanical factors : tensile and tear strength, maximum elongation, elastic modulus. The tensile strength is considered as it represent the limit of stress the material can endure before any permanent damage. The tear strength is overlooked as well as it is better to have a material that resist to the growth of a fracture.

These parameters are important as, at use, the device need to resist and keep its mechanical properties even after manipulations, for example a surgical implantation. The two providers for medical grade silicones are Elkem with the Silbione® LSR silicones [16] Biomedical LSR and Nusil™ with the LSR-MED silicones [17].

As a part of the project my predecessors Margaux Roulet and James Bourely made first researches on the subject. Mrs. Roulet compared the mechanical and electromechanical characteristics of the Sylgard 184© with Silbione® M130 and Nusil™ as shown on Figure 10.

PDMS	Young Modulus [MPa]	Std %	Max Elongation Rate [%]	Std %	Tensile Strength [MPa]	Std %	Tear Strength [kPa]	Std %
Sylgard 184	1.7719	2.3	122.93	3.6	5.0292	2.6	1.6479	13.8
Nusil MED 6215	1.5842	4.7	138.34	5.1	6.2255	1.1	1.8787	6.3
Silbione Bio M130	0.7344	3.4	499.92	8.9	6.5385	12	4.6462	19.9

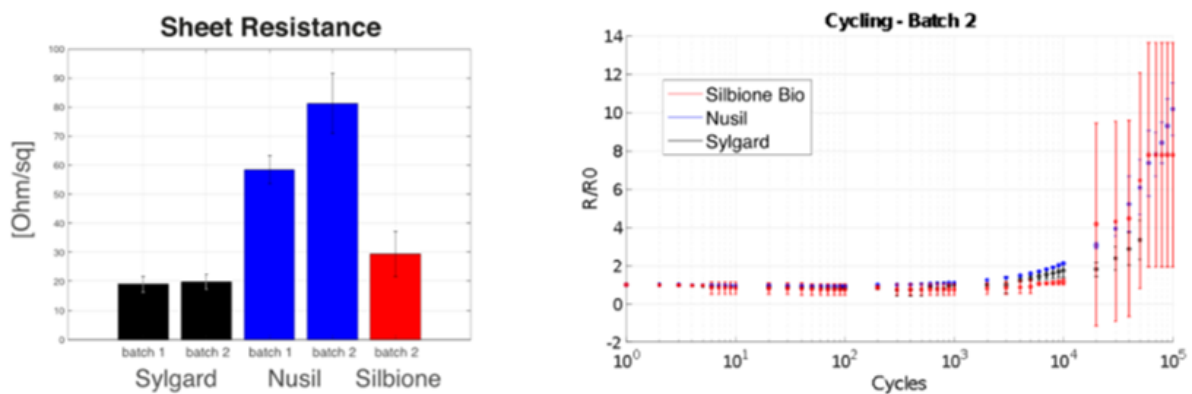


Figure 10 : Data on silicones comparison, M. Roulet(property of LSBI)

As one can see the medical grade silicones present rather good mechanical and electrical characteristics.

Then Mr. Bourely studied the incorporation of the medical grade silicones in the fabrication process. He tested and adapted the coating technic of the silicone, and studied its homogeneity. He also realized a first electromechanical characterization on the Silbione® Bio LSR M130, tested the adhesion between

silicone stacks. Some of his preliminary work and data is on Figure 11 Erreur ! Source du renvoi introuvable..

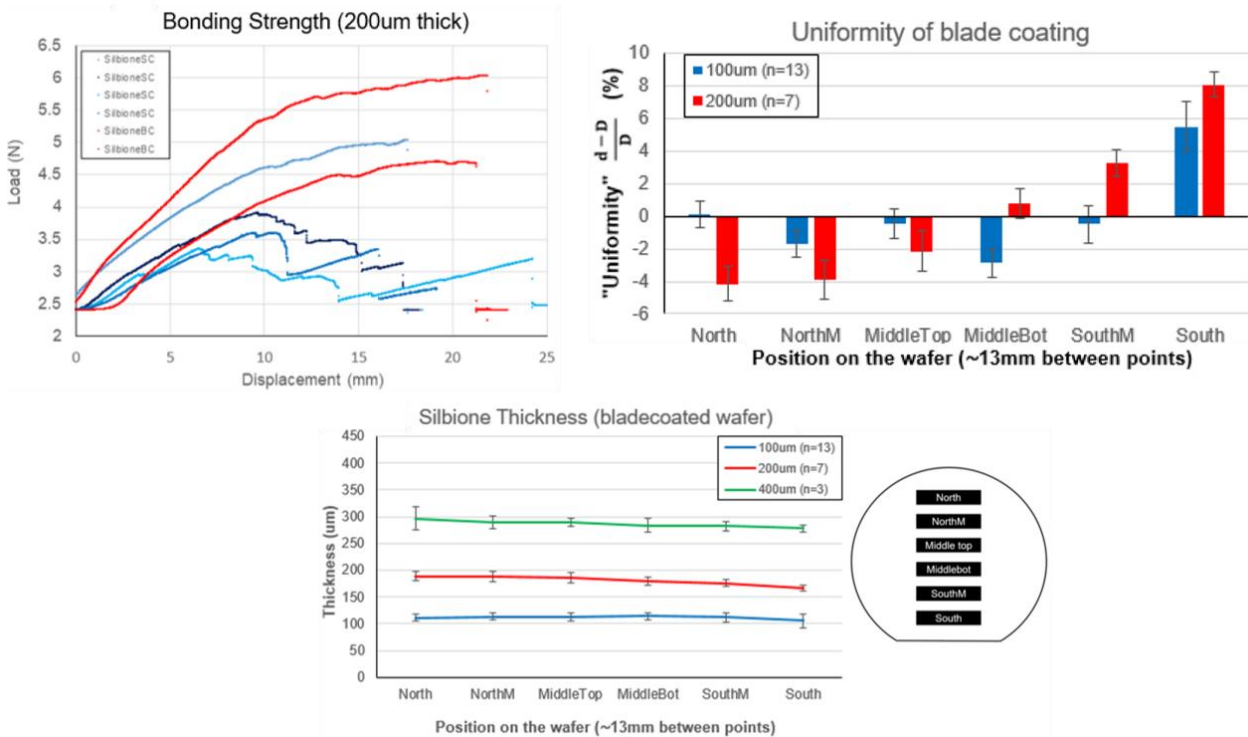


Figure 11 : Multiple examples of previous improvement on materials, J. Bourelly [18] (property of LSBI)

The adhesion between silicone stacks is referred to as Bonding strength in the graph presented by Mr. Bourelly. It is the starting point of one of the main focus of this report, as it goes towards the characterization of the hermetic encapsulation of the device. The encapsulation is currently realized by bonding the top and bottom layers of silicones that sandwich the gold tracks (consider Figure 6). The bond is allowed by an oxygen plasma.

2.2.2.2 Effects of the plasma for the bonding

Oxygen plasma allows to create a covalent bonding between two PDMS layers as shown in Figure 12.

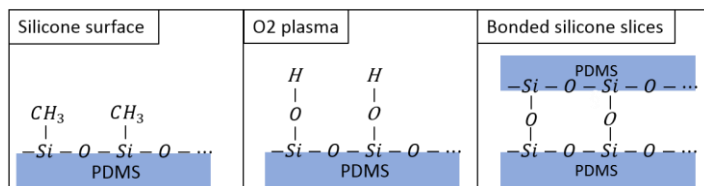


Figure 12 : Plasma bonding schematic

By oxidizing the surface of the PDMS, a silanol layer is introduced (Si-OH), replacing the methyl groups (Si-CH3). The surface therefore becomes hydrophilic, allowing a covalent bonding [19].

Through the years only few studies were conducted on PDMS-PDMS bonding, further more through different technics. For instance Bhattacharya et al. (2005) and Lu et al. (2007) [20] [21] describe the blister test, through which the pressure and the mechanical displacement are observed as shown in Figure 13. The working principle is that the pressure is measured up until the two PDMS layers de-bond, thus giving the maximum pressure, which can be computed as energy of adhesion. Eddings et al. (2008) [22] propose a rather similar test but using only the pressure measured on a specific inlet form.

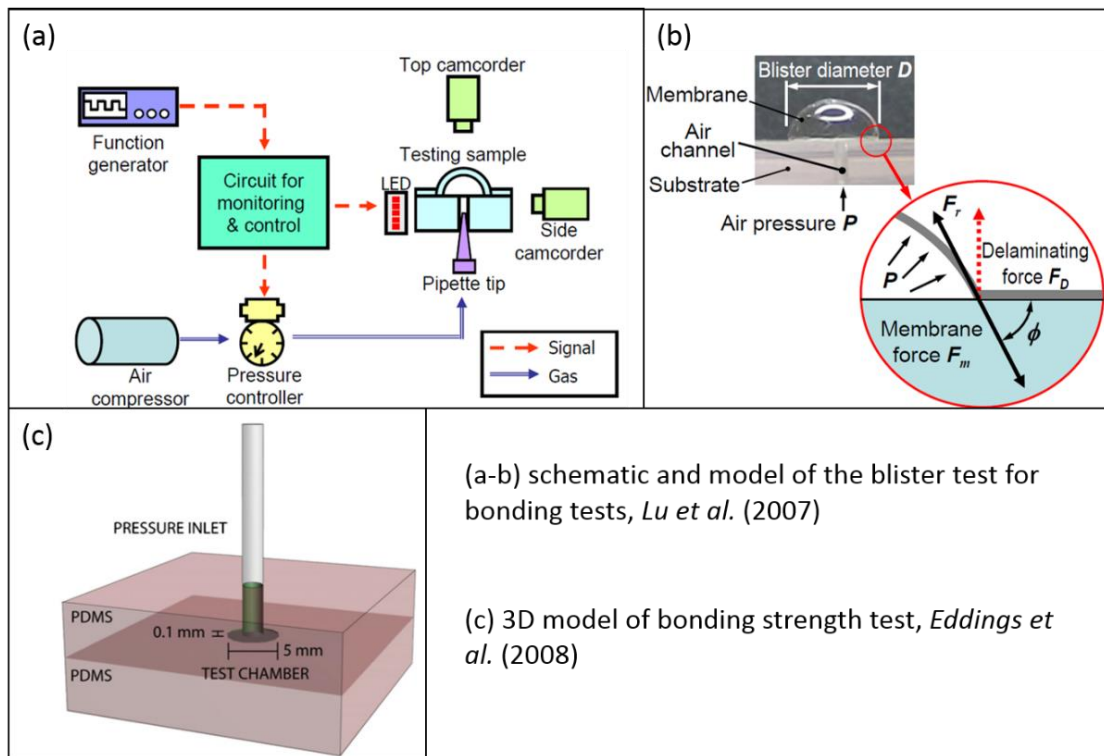


Figure 13 : Bonding strength tests examples [21] [23]

However these tests are not easy to realize. In the case of the Blister test the angle observation is not quite easy to determine if one is not in possession of a proper observation material such as a precise camera with the right angle ; as for the model proposed by Eddings et al., it seems to require a large amount of material to create a sufficiently bulky layer. Moreover no theoretical model is provided which makes it difficult to propose a comparison with practical tests.

Because it demands fewer amount of material and less observation tools, the bonding strength tests are realized through peeling tests. The principle is to peel two PDMS slices bonded together, resulting whether in the silicone to break or on the bonding to delaminate.

Through this test Mr James Bourely concluded that in order to improve the bonding the process could be modify by applying a weigh to the silicones stacks during a 30min 75°C curing in oven, though it is not specified how much the bonding is improved.

2.2.2.3 Adhesion energy

Through the bonding tests, we are trying to look at the energy of adhesion between two stacks of silicone. However the type of test and the dimensions of the samples are key factors if we want to compare our results with the ones we could find in the literature. Eitner et al. (2014) [22] explains, with the schematic on Figure 14, the force induced in peeling tests and the nomenclature of such experiments.

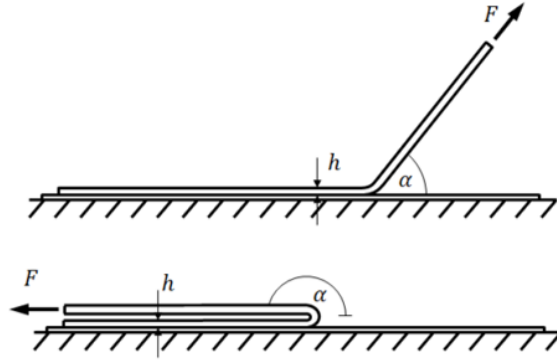


Figure 14 : Peeling test model, Eitner et al.

The external energy that should be computed for such test is therefore

$$G_{ext} = \frac{F}{b} (1 + \varepsilon - \cos \alpha) \quad (1)$$

where F is the load (in N), b the width of the sample, ε the strain and α the angle between each “separated” sample (so 180° for the T-peel test). The external energy is one of those that compose the actual adhesion energy

$$G_a = G_{ext} - G_S - G_T - G_B \quad (2)$$

in which G_S is the stored strain energy, G_T the dissipated energy by plastic deformation and G_B the dissipated energy by plastic bending deformation at the peel front. Now even if Eitner et al. provide a model to compute G_S and G_T , from the material we have it would be difficult to be certain of the strain and deformation endured by the silicones samples during the peeling.

Therefore we computed the energy by using the area below the curve when we measure the load on the displacement of the clamps. This is valid only in the case of an adhesive failure.

2.2.2.4 Aging and accelerated aging

Once they are implanted, subdural electrodes are soaking in body fluids. There could therefore be an effect of those body fluids on the hermeticity of the encapsulation. A consideration of this project was therefore the effects of a Phosphate-Buffered Saline (PBS) solution (often used in biology as its ion and osmolarity composition mirror the ones of a human body) on the bonding of silicone stacks through time.

Moreover, in order to gain time, one would find a way to accelerate the ageing process. The hypothesis on the accelerated aging is that, following the 10-degree rule of Arrhenius’s law, the **aging rate** would increase such as equation (3), with A the aging rate.

$$A_{accelerated} = A_{initial} * 2^{\frac{[T_2-T_1]}{10}} \quad [24] \quad (3)$$

By following this law the aging rate would be of

$$A_{accelerated} = A_{initial} * 2^{\frac{30}{10}} = A_{initial} * 8 \quad (4)$$

Therefore the hypothesis is that for 1week in the 37°C oven the aging effects should be the same on a sample after 21h in the 67°C oven.

2.3 MATERIALS AND METHOD

2.3.1 Types of silicones

The academic silicone we used to compare the medical grade silicones is the Sylgard 184© by Dow Corning.

As for the medical grade silicones, there are the Silbione® Bio LSR 10:1 M130 and Bio LSR 1:1 M140 provided by Elkem, and the Nusil™ MED-4210 and MED-4211 provided by Nusil™. Those silicones were selected depending on their viscosity (75'000cP – 100'000cP) which make them compatible with the E-dura fabrication process, but most importantly as they can be considered for human implantation for a period of <30 days [17] [16]. As explained in the theoretical chapter above, mechanical characteristics of the materials are considered as well. An overview of these characteristics, are given in the following table.

Type of silicone	Tensile strength (psi)	Elongation (%)	Tear strength (Ppi)
Sylgard 184©	980	100	14.7
Silbione® Bio M130	650	480	70
Silbione® Bio M140	975	385	145
Nusil™ MED-4210	1'050	450	100
Nusil™ MED-4211	685	530	-

Tableau 2 : Mechanical properties of the different silicone tested [16] [17] [25]

2.3.2 Fabrication of silicone

The fabrication of the silicone stack is realized on wafers. A first layer of Poly(4-styrenesulfonate) (PSS), that is used as a release layer, is spincoated (@2000rpm). Once the PSS layer is cured, the silicone is spincoated (if Sylgard 184©) or blade coated (Silbione® or Nusil™) for a final thickness of approximately 200µm (±10%).

The silicone is then cured in a 75°C oven for 4 hours. Once cured the silicone is covered by a PET sheet (to avoid deposition of dust on the surface).

Further details on the fabrication steps are given in annexes (A2).

2.3.3 Bonding test

2.3.3.1 Samples fabrication

The silicone layer, protected by the PET sheet, is laser-cutted in rectangles (10mm × 30mm).

Then the silicone stacks are bonded together, as shown in Figure 15, by sandwiching two stacks of silicone, after having activated their surface with an oxygen plasma. Half of the interface is covered by a PET sheet, to avoid the bonding of the entire surface.

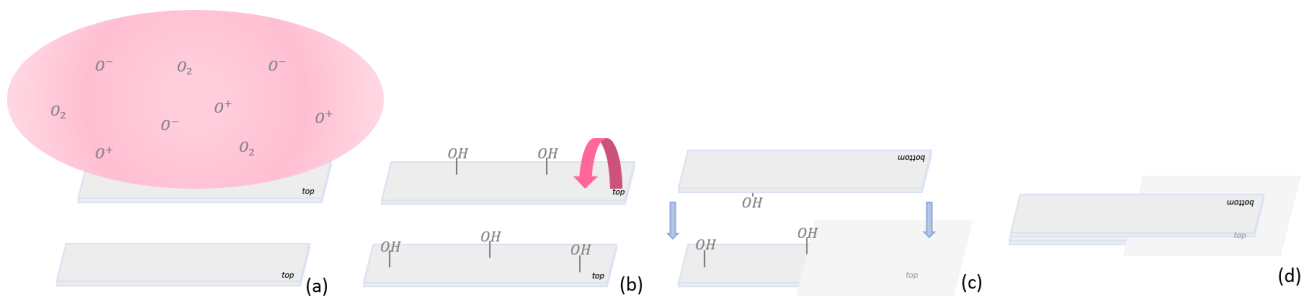


Figure 15 : Plasma bonding steps (a)Surface activation through plasma (b-c)Flipping one slice to go on top of the other, with a PET sheet to protect half of the slice to bond and (d)the final bonded sample

The plasma recipe has been proposed by Mr Bourely from literature (Oxygen plasma, 0.2mbar, 5sccmO₂, 60W for 1min) ; as it has been recognized as the most efficient recipe from previous work it has been taken in this project as such.

2.3.3.2 T-peel test

The bonding test is performed by a T-peel test as presented on the Figure 16 **Erreur ! Source du renvoi introuvable.**, on which the material dimensions and the set-up are presented. The peeling speed is of 0.5mm/s for observation purpose.

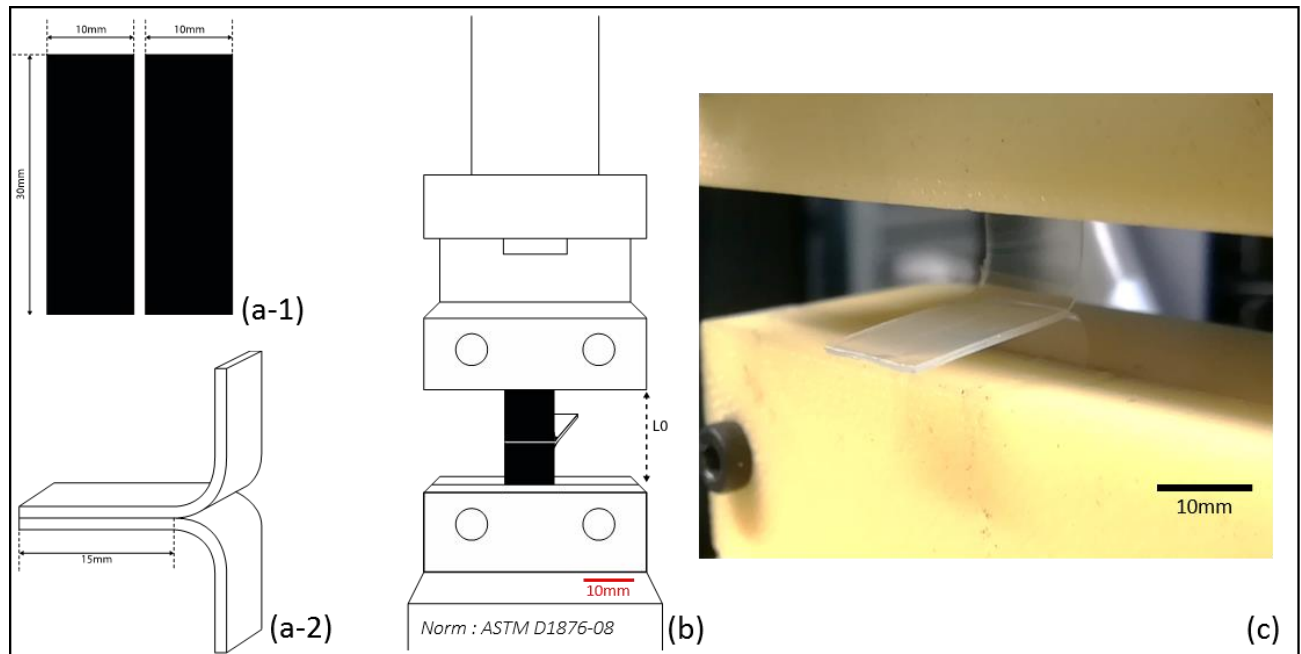


Figure 16 : T-peel experiment for bonding test schematic (a-1)Dimensions of silicones samples (a-2) T-peel test positioning of the samples (b) Stacks installed in clamps and (c)Picture of installed samples

Both silicone stacks have a non-bonded part, as it was protected by a PET sheet as on Figure 15. Each of those non-bonded part will fixed in clamps, closed on the silicone by two screws. In order to prevent the stacks from sliding, a small piece of sandpaper is placed between the silicone and the clamp. The operator placing the silicone has to be careful to properly align the silicone samples. Moreover the clamps have to be installed as close as possible for each other, to reduce the length of the silicone samples that might elastically deform and that we do not wish to observe. Then the clamps should be positioned from each other to allow the sample to be taut. Finally, on the software, the position of the clamps has to be set to zero, to measure the actual elongation during the T-peel test.

The bonding test is showed as the load applied depending on the displacement of the clamps from each other (which is referred to as *Elongation* on the graph) as shown on the example on Figure 17.

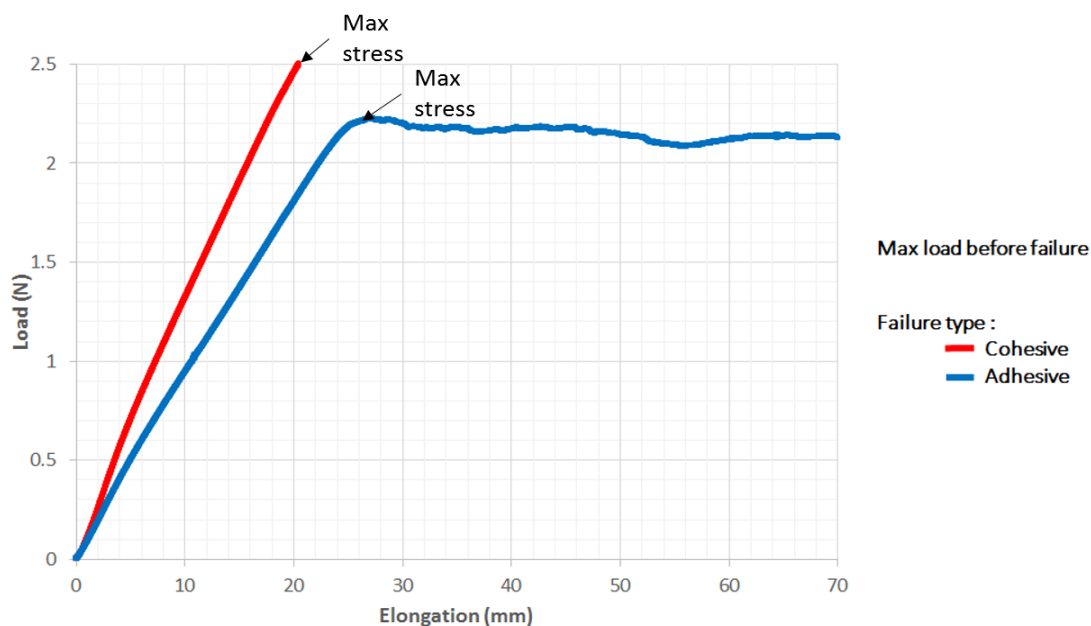


Figure 17 : Typical output to expect during a bonding test of peeling force on the elongation, the blue curve indicate a cohesive failure, while the red curve indicate an adhesive failure

As one can see from the graph there are two main output from the test : in the case that the fragility of the silicone is more important than the bonding between the two stacks, one of the stacks will break ; this is referred to as a **cohesive failure**. On the other hand if the silicone stacks peel-off from one another rather than breaking we will talk about an **adhesive failure**. In the case of a cohesive failure the maximum point reached mirror the ductility of the material and **not the adhesion**, it will therefore not be assimilated to an adhesion energy.

On the other hand the flat region of the red curve indicate a delamination of the samples, which can be assimilated to an adhesive energy.

Bonding tests allow us to compare mechanical properties between Sylgard 184© and medical grade materials, here Silbione® M140 as it was the main available resource.

Through the bonding test it is also possible to observe the degradation of the bonding through time.

Exclusion criteria of the bonding tests :

Some samples can have an odd behavior while being stretched and they are sometimes considers as not relevant in the study.

For examples some samples will present a cohesive failure for a very low energy when compared to other samples (more than 40% difference). As the samples are bonded by hand, it can therefore be considered a human error and are therefore not considered in the graphs and results presented in this report.

2.3.4 Stiff backing

In order to observe differently the bonding strength of the silicone stacks, other T-peel tests were realized with materials used to rigidify the silicone stacks.

The samples of stiffen silicone stacks are the same dimensions as for a simple bonding test (consider Figure 16).

We tried three type of stiff backing :

- PET bonded to the stack with plasma ; the silicone was actually blade-coated on the plasma activated surface of the PET, for the silicone to cure on the PET sheet.
- PET fixed with RTV ; were here the PET sheet will be added on the bottom of the silicone stack and only plasma bonded, and fixed with RTV poured on the edges of the PET sheet.
- Tape backing ; following the proposition of Hoang et al. [26] one surface of the silicone stack was activated through oxygen plasma and the tape was disposed on this exact surface.

A clearer illustration is presented in Figure 18

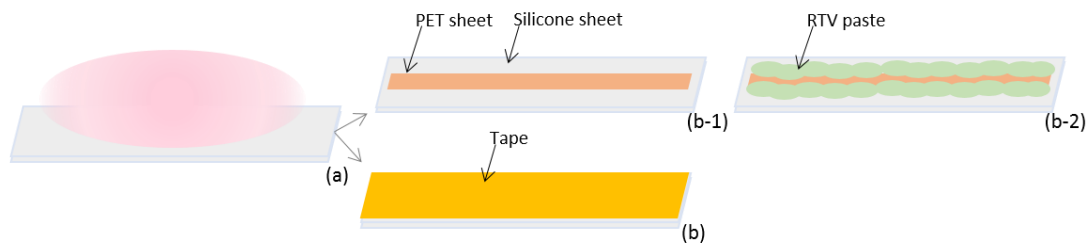


Figure 18 : Schematic of the fabrication of stiff backing samples, in (a) the oxygen plasma activation of the surface, then (b.1-2) use of PET sheet fixed with RTV and (c) tape (Kapton) application

In the context of its use the device, if implanted for a period of time up to 30 days will be soaking in body fluids present around the brain. In order to ensure the survival of the device in such liquid one has to test the interaction between the device, its encapsulation and a solution which would present similar properties as those body fluids. That is the purpose of the following aging tests.

2.3.5 Aging tests

To verify the effects of time on the adhesion between silicones stacks and to be closer to the model of an implant, peeling tests are realized through time for bonded samples soaking in a Phosphate-Buffered Saline (PBS) solution (solution often used in biology as its ion and osmolarity composition mirror the ones of a human body) in an oven of 37°C to be close to the average body temperature. A schematic of the soaking sample is available on Figure 19.

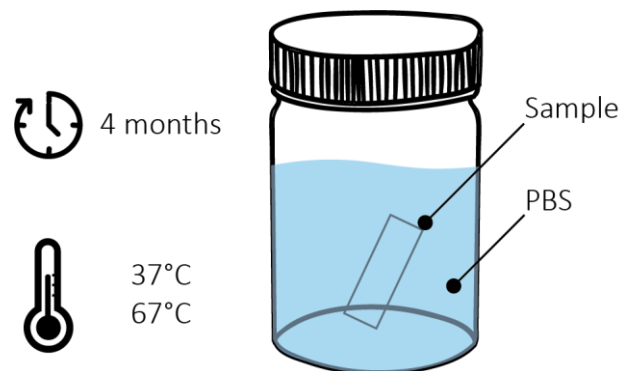


Figure 19 : Accelerated aging sample example, soaking up until 4 months, at 2 temperatures

The aging is verified through T-peel tests, where we observe if there is an evolution in the necessary load for cohesive/adhesive failure.

The expected output is to observe a significant change in the necessary load to de-bond the silicone stacks.

Moreover for the **accelerated aging test**, soaking samples were placed in PBS solution, in a 67°C oven, for the equivalent time-stamps as the ones for the 37°C aging test.

Exclusion criteria of aging samples :

It might occur during the test that some samples show a completely different behavior than the others. As the slices are disposed on each other by an operator with few control over the precision of alignment, it has to be considered in the conclusion of the test that a misplacement of a silicone slice would be the origin of unexpected behavior. All data is however considered.

2.3.6 Electromechanical characterization

The electromechanical characterization aim to characterize the behavior of the electrical resistance of the gold tracks while stretching. As showed in Figure 6, the gold tracks are sandwiched between two layers of silicone of 200 μ m each. The typical form of a sample is the schematic of Figure 20-a. This design allows us to connect ZIF on each side and measure the impedance from both ends of the gold tracks. On Figure 20-b the arrangement of samples on wafers. The numbering and the order of numbering is important as the quality of fabrication is verified through the electromechanical characterization, which is realized sometimes later on by the operator.

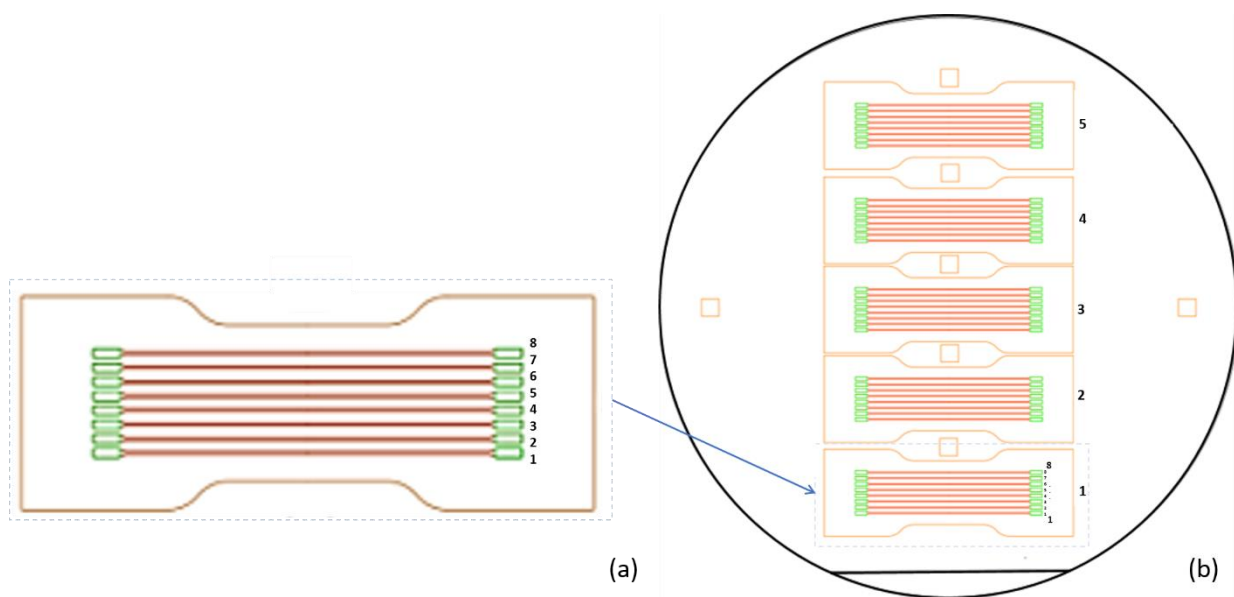


Figure 20 : (a)Example of sample to be stretched and (b)example of arrangement of samples and strips on the wafer

For the electromechanical characterization, the first step is to measure the resistance of the full fabricated device when it is still on the wafer , what will be called **sheet resistance**. The sheet resistance gives the non-stretched resistance of the gold track, and it can change depending on the silicone on which it is deposited. Then samples undergoes **stretching and relaxing cycles** to allows us to observe the fatigue of a full device, such as the survival of a conduction path in the gold tracks allowing an electrical conduction.

As shown on Figure 21, resistance of the tracks is measurement with a *Fluke 115 True-RMS Digital Multimeter*®. Measured resistance shall be of the order of the kilo Ohm.

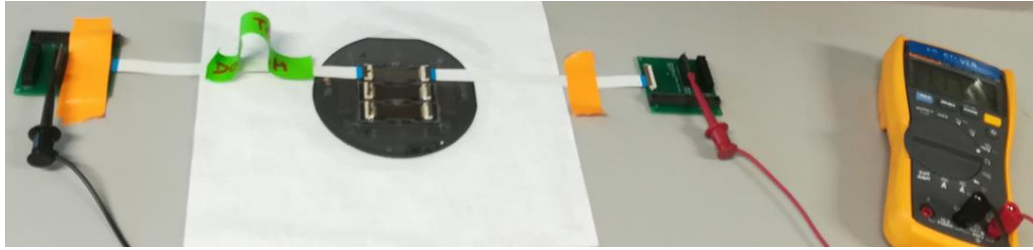


Figure 21 : Sheet resistance measurement set-up

The Figure 22 shows the main parts that compose the electromechanical characterization. The linear movement is realized by an eccentric system, on which it is possible to fix the radius of the motors rotation, so it is possible to adapt for each sample the elongation depending on its initial length (which can change of a few micrometers).

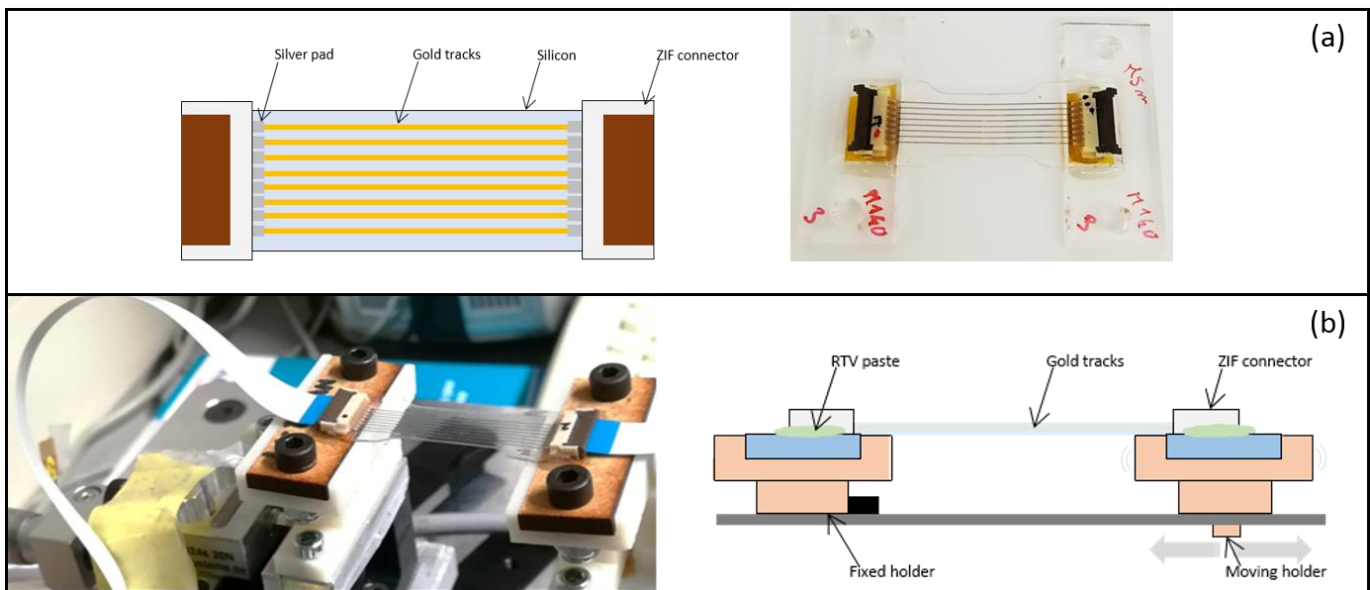


Figure 22 : Electromechanical characterization schematics and pictures;
 (a) Sample to be stretched (x) composed of 8 gold tracks (n) (b) Set-up (main pieces)

Both the silicones stacks and a part of the ZIF (Zero Induced Force) connector are fixed to Polymethyl methacrylate (PMMA) or wood aligners, otherwise the connection between the ZIF connector and the gold tracks, through the silver paste, could break during the stretching.

The stretcher elongate at a frequency of **1 Hz**. During the cycles the electrical resistance of the tracks is measured and noted in a text file, which allows us to observe rather easily the evolution of the resistance through said cycles. As seen in the introduction (Figure 9) this evolution of resistance is then computed and plot as the **normalized resistance R/R_0** . R_0 is the first minimum resistance measured at the beginning of the stretching cycles, when the sample is at rest, so when the elongation is at 0%. What is plotted is the average measured resistance on R_0 for each cycle.

The aim of this test is first to compare resistance evolution of medical grade silicones (Silbione® by Elkem, Nusil™) with academic silicone (Sylgard 184©), and then to obtain more knowledge on the electromechanical characteristics of the material. What is wished to be observed is an as small resistance change as possible though the cycles.

Exclusion criteria of electromechanical characterization :

It is important to measure the sheet resistance before freeing the samples from the wafer in order to have as few changes as possible in the gold tracks. Similarly the ZIF connectors, as fixed with RTV silicone on the side, can easily get ripped off the sample. It is therefore one of the main issues regarding the yield of the device full fabrication.

We make a distinction between a connection problem due to the ZIF displacement and a broken/unworking gold track, because a ZIF displacement is often due to a mis-manipulation of the device once it is fabricated while a problem with the gold tracks often means that there is an issue in the fabrication process.

In the results the distinction is made, where **n** will be the total amount of **working tracks** and **x** the total **number of samples** tested. If we take the example of the Figure 20, there are 5 samples on each wafer, for 8 tracks per sample.

2.4 RESULTS AND DISCUSSION

This section of the report will focus on analyzing the data gathered during the experiments. We will interpret them and draw conclusions, as well as plan further experiments.

2.4.1 Bonding tests

As a reminder, the hermetic encapsulation verification plays a role in both ensuring patient safety and continuous electrical conductivity during an implantation time up to 31 days.

On Figure 23 academic and medical grade silicones bonding strength are compared.

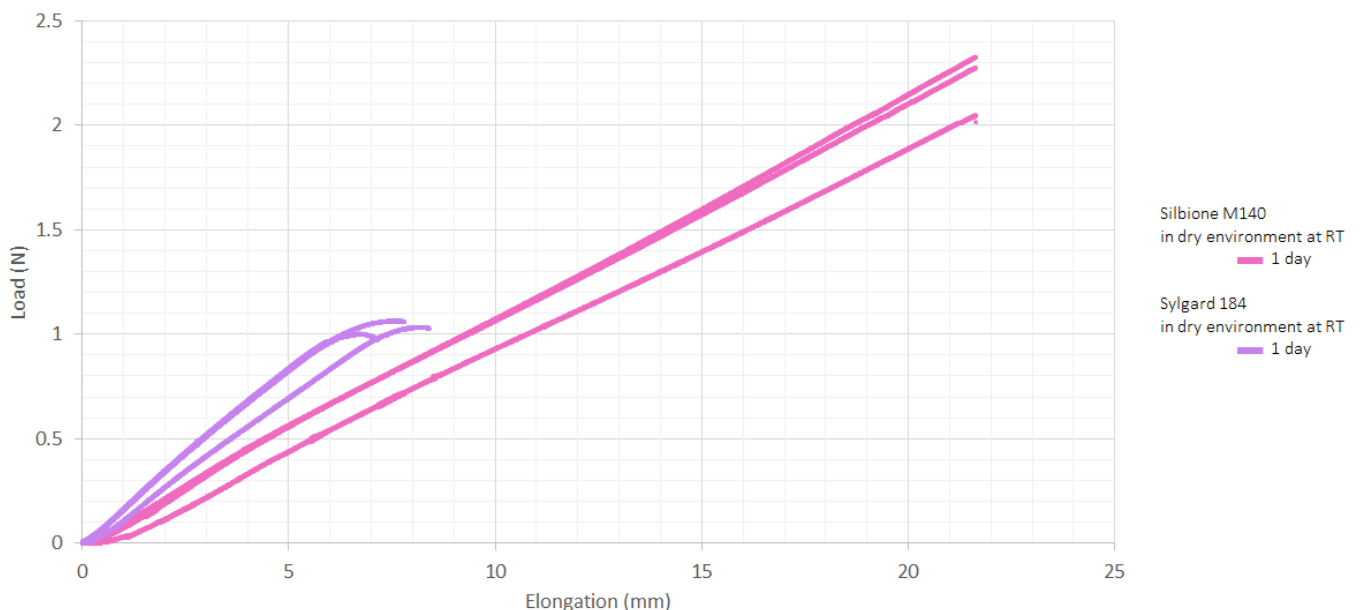


Figure 23 : Bonding test of Sylgard 184© samples (purple, n=4) and Silbione® M140 1day after plasma (pink, n=3)

From this graph one can see that the Sylgard 184© collapses for a smaller force than the Silbione® M140.

Sylgard samples present the beginning of a flat before breaking, meaning that they started to delaminate just before breaking. This would mean that apart from the fragility of the silicone this energy would be the point of adhesive failure for the Sylgard©.

Silbione®M140 samples on the other hand can handle a much higher force before breaking and without showing signs of adhesive failure.

From these results we understood that what we are looking at during a cohesive failure is the mechanical ductility of the materials and therefore not the adhesion energy by proper meaning. From this and regarding the literature we decided to try to observe the real adhesion energy without observing the elastic deformation of the silicone. We therefore tried to make tests with a more rigid backing on the samples.

2.4.1.1 *Stiff backing*

Stiffening the back of the samples would ideally cancel/prevent the elastic deformation of the silicone stack, giving as a result a graph showing the force growing only due to the adhesion of the samples. However the stiff backing would peel-off the back of the sample (as shown on Figure 24), making the use of it pointless. Nonetheless, interesting insight can be drawn from those tests.

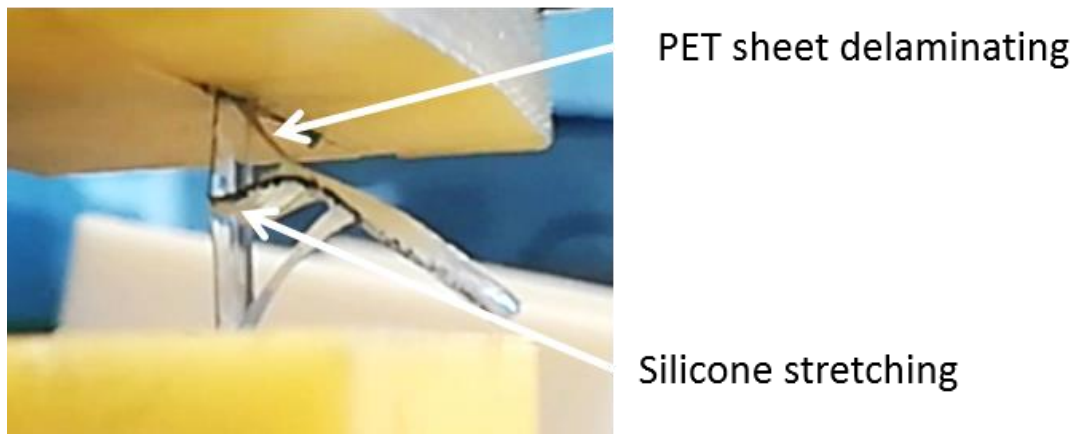


Figure 24 : Stiff-backing T-peel test

The first tests realized were with only a PET layer bonded with the silicone stack with a plasma activation. However the PET detached easily, so we tried backing with PET fixed with RTV after a plasma activation on the surface of the stack. Finally we tried backing with tape. For clarity only one material, the Silbione[®] M140, has been tested for the stiff backing experiments.

On the following graph one can see all the curves of the samples tested (Figure 25).

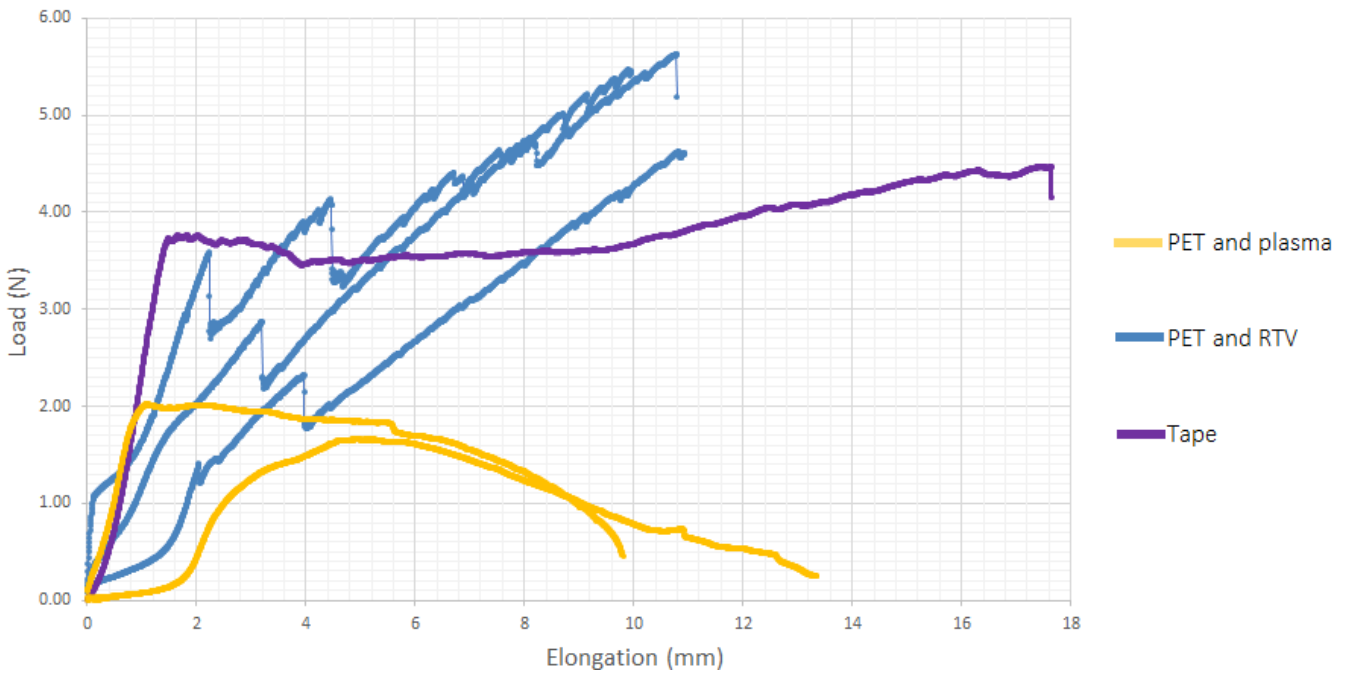


Figure 25 : Stiff-backing bonding tests of Silbione® M140, with PET bonded with plasma (yellow, n=2), PET fixed with RTV (blue, n=3) and adhesive tape (purple, n=1)

The PET fixed with plasma (*PET and plasma* on the graph) detached early during the stretching, therefore the yellow curves show a maximum energy very close to the one we find in a regular (no stiff backing) test (consider following Tableau 3).

The PET fixed with RTV show steps (sudden drops of load applied) which is due to the detachment of PET and RTV from the silicone stack.

Types of backing	Maximum load (N)
Without stiff backing (highest energy measured, 1w aging)	2.78
PET and plasma	2.02
PET and RTV	5.63
Tape	4.47

Tableau 3: Maximum load and energy from bonding tests, from *Erreur ! Source du renvoi introuvable.* and Figure 26

The fixation realized with tape shows a plateau, that formed because of the tape delaminated from the silicone. Hence it still did not allow to observe completely the delamination of the silicone-silicone bonding, but rather the tape-silicone bonding.

There are however two important things to notice from these results. The first thing is that those tests are not reliable to observe an adhesion energy, as we still observe the elastic behavior from the material. The second is that the maximum loads applied on those samples are more than two times higher than the ones observed without stiff backing. This would mean that even if we are not yet observing the adhesion energy itself, at least one component of the simple T-peel tests, the ductility of the material, is compensated by the reinforcement of the sample through the backing material. Therefore where we previously had a cohesive failure we might now be able to observe for a higher load applied the bonding of the sample, getting closer to the real force needed to delaminate the stacks from one another.

2.4.2 Aging process

Once slices have been cut and that the surface have been activated by oxygen plasma, the two slices are bonded together and let to soak in the PBS solution for as long as we could still have slices.

The first graph shows a comparison between bonded Silbione® M140 silicone slices 1 day, 1, 2 weeks and 4 months after plasma soaking in a PBS solution at 37°C (Figure 26).

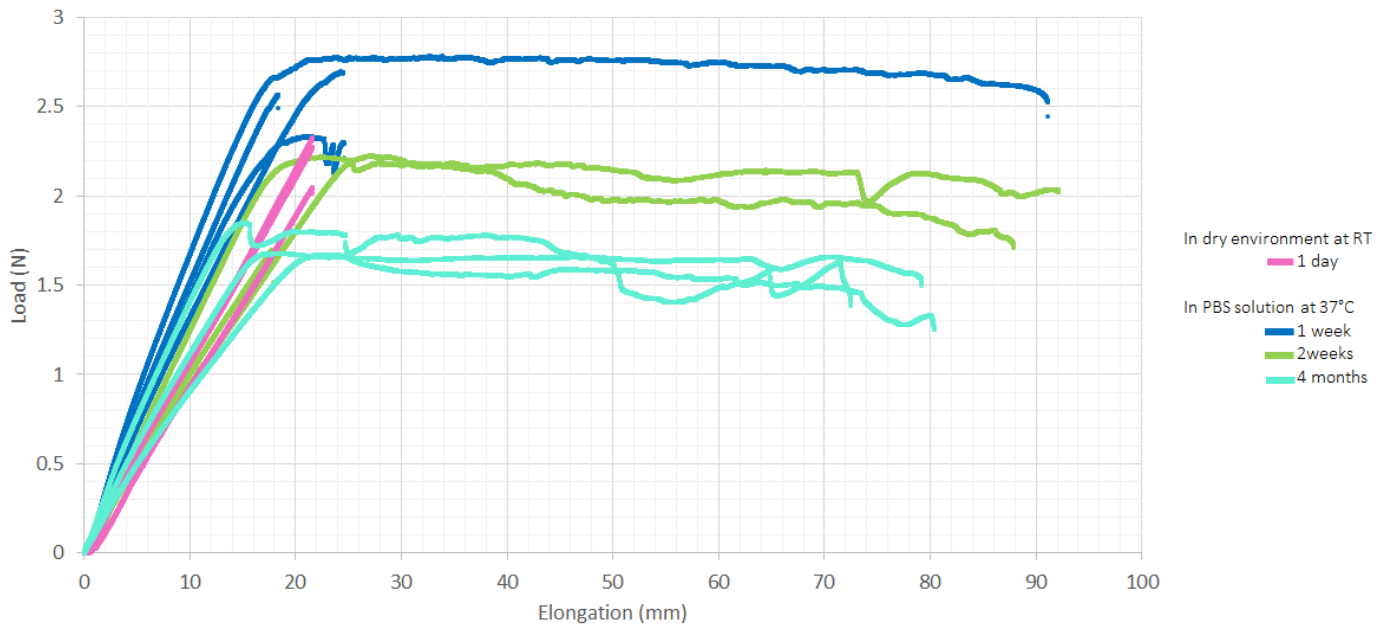


Figure 26 : Bonding test on Silbione® M140 1day after plasma (pink, n=3), 1week after plasma in PBS solution at 37°C (blue, n=4), 2 weeks after plasma in PBS solution at 37°C (green, n=3) and 4 months after plasma (clear-blue, n=3)

As one can see after 1 week of soaking, only one sample de-bond while three others present a cohesive failure. This result can be explained by two hypothesis. The first one would be a mis-alignment between the PET sheet and the slices of silicone, as explained in the chapter 2.3.5. The second possibility is that the 1 week aging is at the limit between the permanent cohesive failure observed at 1 day of bonding and adhesive failure.

The fact that the adhesion failure occurs with a lower energy after 2 weeks shows that there is an effect through time of the aging in the PBS solution. The aging is therefore to be consider as it might degrade the hermetic encapsulation over time.

Aging time	Maximum load (N)	Energy (mJ)
1 day	2.33	-
1 week	2.78	194.6
2 weeks	2.23	144.95
4 months	1.85	120.25

Tableau 4 : Maximum force and energy for each aging period

The preparation of samples require a certain amount of time and material which is the reason of the few amount of time stamps. For our interest we however kept 3 remaining samples in the PBS solution at 37°C for 4 months.

From these aging test we see that there is an evolution of the type of failure and the force needed to de-bond silicone stack from each other. This test is therefore conclusive on the observation on aging on bonding of silicone stacks. However, there is a higher load required to break or delaminate the samples after 1 week, which mean there is also an effect on the elasticity of the material. This should be investigated in another project.

In parallel we tested the same samples in other aging condition.

2.4.2.1 Accelerated aging test

Here we compare the same materials under the same circumstance but the temperature of aging which was of 37°C for some samples and of 67°C for some others. The following graph show the T-peel tests of each of these samples.

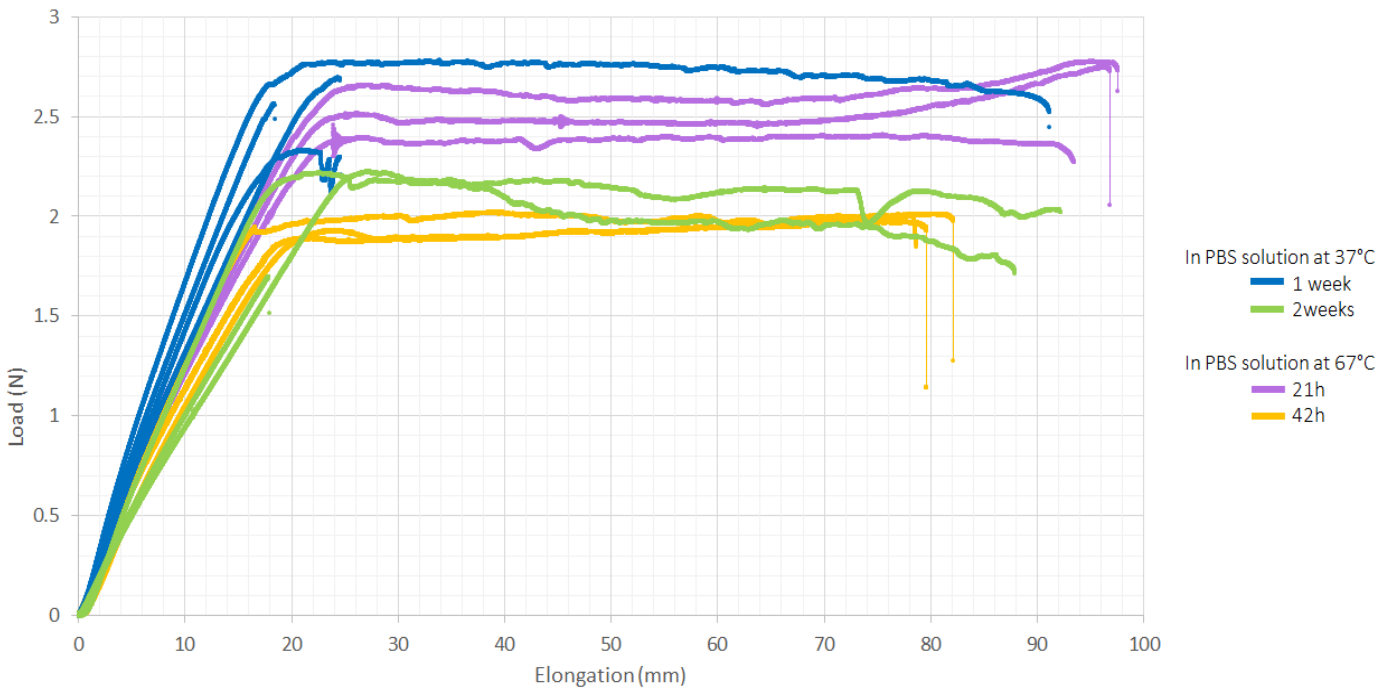


Figure 27 : Accelerated aging test following Arrhenius law [24]

The equivalent time-stamps are highlighted in Tableau 5 computed with equation (4).

37°C	67°C
1 week	21 hours
2 weeks	42 hours

Tableau 5 : Accelerated aging equivalent time-stamps

From the graphs of Figure 27 one can see that the evolution of delamination force needed depending for the same equivalent time is rather similar, the Tableau 6 summarize through the highest de-bonding loads the similarity of those curves.

	37°C	67°C
1 week / 21h	2.78 N (194.6 mJ)	2.78 N (194.6 mJ)
2 weeks / 42h	2.23 N (144.95 mJ)	2.03 N (121.8 mJ)

Tableau 6 : Comparison of the maximum load depending of the aging temperature

Even if these aging results seem almost identical, the fact that after 1 week in the 37°C PBS solution 3 samples out of 4 present a cohesive failure while for the equivalent aging condition samples in the 67°C PBS present an adhesive failure make the equivalence of aging doubtful.

If we isolate the adhesive failure curves, we find a similarity between the two aging technics, for a difference in the maximum load of approximately 10%.

Whilst these results are promising, we cannot conclude a one to one correlation between fast aging samples and standard aging samples. It is needed to first, have more samples per time-stamps and second, conduct the experiment with more time-stamps to validate this method.

2.4.3 Electromechanical characterization

The electromechanical characterization is crucial to determine the abilities of the materials to implement.

The two main factors through which we determine which materials is better than another is its initial resistance and the lasting of the gold tracks through stretching.

On the Figure 28 one can see the plot of the normalized resistance through cycling of each materials tested. Graphs of each materials can be seen in Annexe (A2).

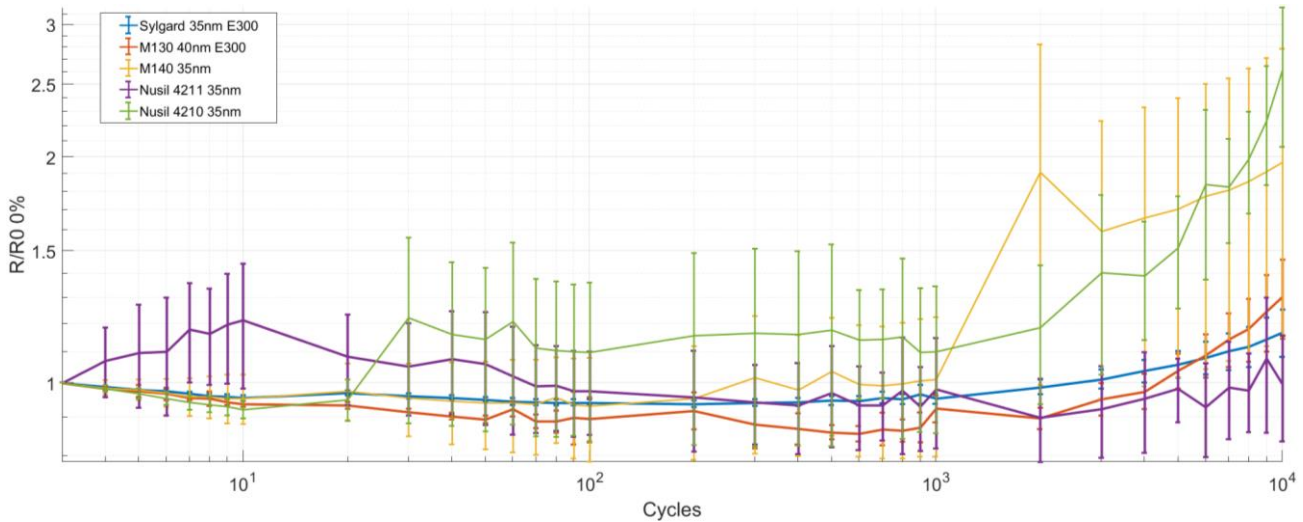


Figure 28 : Normalized resistances of all materials (avg+std on n tracks), Sylgard 184 (blue), Silbione® M130 (orange), Silbione® M140 (yellow), Nusil™ 4211 (purple) and Nusil™ 4210 (green) through electromechanical characterization; each material except for the Silbione®M130 has a gold layer of 35nm

The Nusil™ 4210 and the Silbione® M140 present a fast growing resistance from 1000 cycles, making them less attractive as material for a long term implantation.

Silicone (PDMS) type	Initial Sheet Resistance [Ohm/sq]	n (x)	R/R0 at 10k cycles	Yield
Silbione Bio M130(30nm) n=12	34.11 ± 5.01	12 (3)	1.25 ± 0.025	62.5%
Sylgard 184© Dow Corning n=16	8.23 ± 1.22	16 (2)	1.17 ± 0.084	100%
Silbione© Bio M130(40nm) n=12	28.5 ± 2.605	12 (3)	1.35 ± 0.016	62.5%
Silbione© Bio M140 n=12	13.5 ± 8.58	12 (3)	1.08 ± 0.065	62.5%
Nusil™ MED 4211 n=22	18.78 ± 5.58	22 (3)	1.0 ± 0.160	91.6%
Nusil™ MED 4210 n=7	16.7 ± 1.393	7 (1)	2.36 ± 0.249	87.5%

Tableau 7 : Resistance and sheet resistance of tested materials, except for the Silbione©M130 each samples have track of a gold thickness of 35nm.

From the graph, one can see that Silbione® M130 and Nusil™ 4211 have a resistance evolution similar to the one of the Sylgard 184©. The Silbione® M130 has a higher sheet resistance than the Sylgard 184©, however it is in the same order of magnitude as for the Silbione® M140. It is similar for the Nusil™ 4211 with regard of the Nusil™ 4210, that has an even better yield.

Each medical grade silicone provider has at least one silicone that comply with our requirements towards the use of the Soft ECoG neural implant: the Silbione® M130 for Elkem and the MED-4211 for Nusil™.

2.5 CONCLUSION

The tests we realized on the medical grade silicones give a good insight on their abilities towards their use for the SOFT ECoG.

The aging tests show that there is indeed an effect of the PBS solution through time on the bonding, and that therefore the hermetic encapsulation might not be ensured for an extended period of time. The accelerated aging gives promising results, however it has been determined that, due to the difference of cohesive and adhesive failure on the samples, we could not conclude on the guarantee of valid relation between the aging at 37°C and at 67°C (for equivalent time spent in the PBS solution). One shall reconduct this experiment, but with a higher amount of samples (n=10 ideally) and with more time stamps (2 times a week for 30/31 days).

The stiff backing experiment hasn't been entirely successful as the stiff backing would delaminate from the silicone stack, it however gave some hints for the maximum load required to delaminate the bonded silicone stacks. If someone were to find a stiff back that would remain attached to the silicone, one could study the bonding strength while not being limited by the possible load applied due to a cohesive failure. It would allow to compare from day 0 the bonding energy and draw a conclusion on the effect of aging, furthermore show the maximum time during which such technology could be implanted.

Finally the electromechanical test showed that, for the two medical grade silicone providers, at least one of them allowed the formation of microcracks and that present good electrical characteristics through stretching.

Although these results are conclusive with respect to the functionality of medical grade silicones, there are missing aspects that do not allow us to make a conclusion as such.

As for the bonding tests, the tests of stiff backing were tested because the T-peel test did not allow to see the strength of adhesion so to speak. Moreover, there is no defined value on the minimum force to be produced for the debonding of the silicone stacks. Thus the experiments give us a global idea of the bonding capacity, but do not allow us to conclude on a final value that would allow us to validate the bonding of the silicone. Because of the lack of a clear definition of the expected results, the tests do not make it possible to definitively conclude on the success of an experiment or, for example, the validation of a material. Finally the translation to clinic require documentation for each step of such experiment, that would allow there approval for clinical use. Such documents do not exists yet for those tests.

Thus, in order for the next test to be decisive in the validation of a new material for the SOFT ECoG, the next chapter is devoted to the explanation of the various aspects allowing the legal validation of a system for a medical use.

3 DESIGN OF PROTOCOLS FOR SYSTEMATIC DEVELOPMENT

The translation to clinic require specific documentation to allow the proper verification of a device. This documentation is also needed to conduct tests as the ones we have seen in the previous part. The tests conducted for such translation aim to show that the device will be safe and reliable once at use. Therefore the design of those tests should mirror as much as possible the conditions in which the device will be once at use.

The following chapters aim to give an overview of the requirements for the translation towards the clinic and to show an example of a test designed to mirror the condition of a device while at use.

3.1 REGULATORY REQUIREMENTS

Since May 2017 the European Medicines Agency introduced Medical Device Regulations (MDR 2017/745), defining the now legal requirements to meet for a device to be considered safe and performant for medical use. The biggest challenge to bring implants for use in the CNS to clinical trials is to enter the framework in which the conception of the device as to go through to be MDR-compliant, requiring all fabrication steps and materials to be adapted, as explained in introduction. Those steps are presented more clearly in the following graph (from Figure 29).

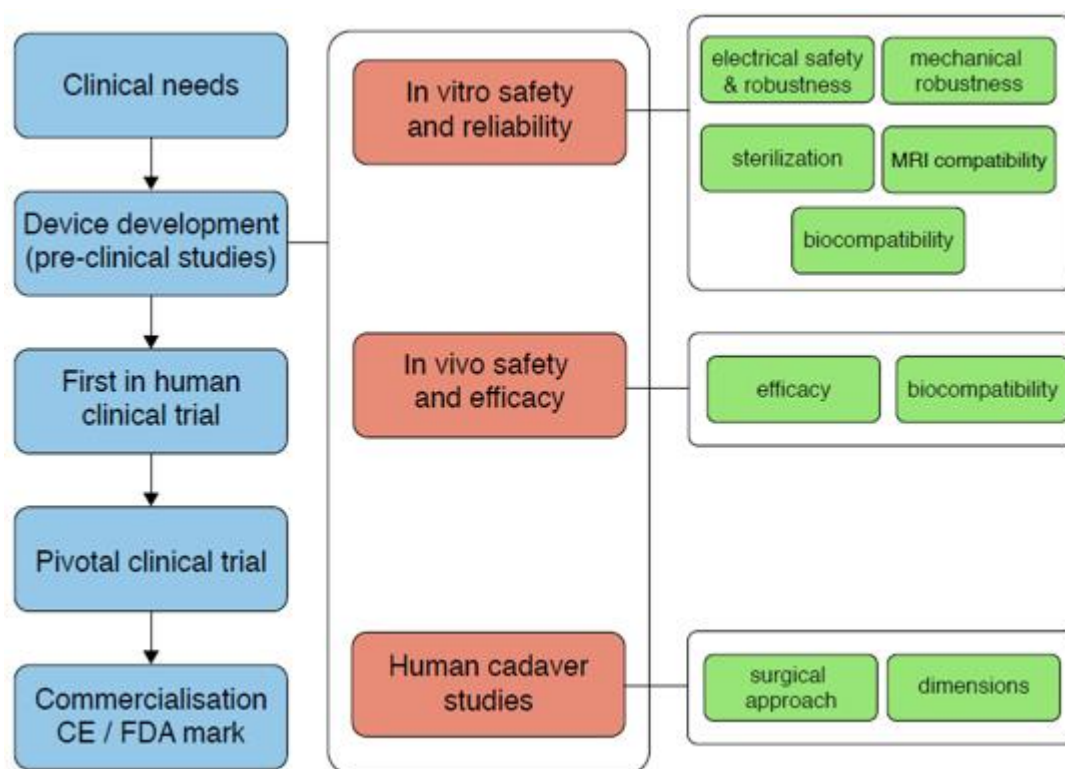


Figure 29 : Roadmap of a clinical device [27] adapted from [28], property of the LSBI

Set standards such as ISO 13485:2016 bring the steps through which to groups and companies that wishes to translate to legally marked medical grade applications have to go through. Regulation requirements are both technical and management-oriented, for ensuring biocompatibility of the device to the paper work around the management of the quality of such tests.

The translation to the clinic can be compartmentalized in two categories: the administrative procedure that allows verification and validation of the systems on one hand, and on the other hand the verification of the biocompatibility and the correct design of the system.

3.1.1 Biocompatibility

Proving the biocompatibility of a device is a hard validation to make as the frame of term is very broad and complex. The general terms encompasses multiple tests to pass:

- Cytotoxicity
- Chronic toxicity
- Sensitization
- Pyrogenicity
- ...

It is also good to keep in mind that the translation to clinic can include many actors which can lead to complex situations. For instance when selecting a medical grade material, the manufacturer (or the organization) has a responsibility towards the provider and *vice-versa*. The provider have to accept to make the tests required for certification of biocompatibility of the material, but they have to be certified to do so as well.

3.1.2 Other soft ECoG clinical translation

The Wise Cortical Strip (WCS) aims to be legally marked by the end of the year and is therefore making the translation towards MDR approval. In a recent patent application publication [29], L. Ravagnan, CEO of Wise highlight some of the requirements of both the manufacturing process and the device itself regarding for example biocompatibility. It is specified in the patent that, even if the materials used for the fabrication are biocompatible, the manufacturing process itself shall not alter the biocompatibility of the device to be obtained. This is a crucial point as each step of the way of the device manufacturing, transportation and handling has to be defined and verified for the device to be legally marked.

3.1.3 Administrative procedure

The market on which the project takes place is the European market and we therefore aim to be legally CE marked (Conformité Européenne), however as most example found in the literature concerns FDA marked devices (USA legislation) some examples are taken from translation towards FDA validation cases. One should however admit that the resemblance in the design and safety principles are sufficient for the link to be made.

To bring a device to its validation on the market each step of its process has to be documented. The following graph, adapted from R. K. Shepherd [30] shows the verification and administrative steps that cover the creation and existence of a device (Figure 30).

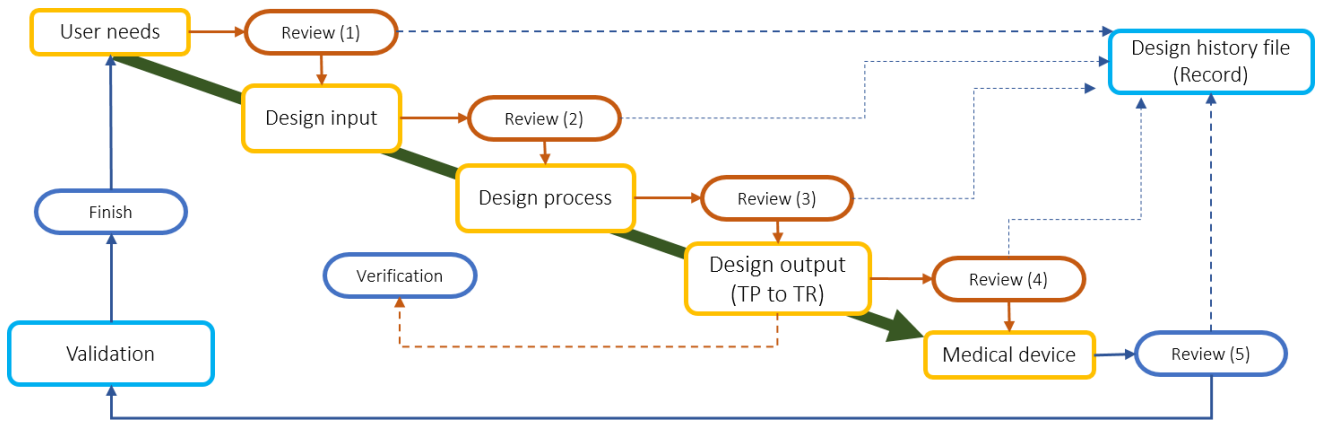


Figure 30 : Adapted from R. K. Shepherd [30], Application of Design Controls to Design process

The Design input shall ensure that the device is design towards the specific needs of the users that meets the requirements of regulation organisms. Design output shall give the acceptance criteria and details the outputs expected for a proper functioning device. Between these steps documented reviews have to be conducted and validated by another operator which would note the history and details of each design parts. Finally, the Verification of the device means to consider if the device meet the expectation listed by the Design input while the Validation of the device aims to consider the use of the device regarding the user’s needs and safety.

A group that wish to make the translation towards legal marking shall pass and documents each of these steps.

In the context of this project, the part in which our experiments take place if the Design outputs. The Design output shall contain also the forms through which a batch or a sample, towards the usage of the device, has to pass (consider Figure 31).

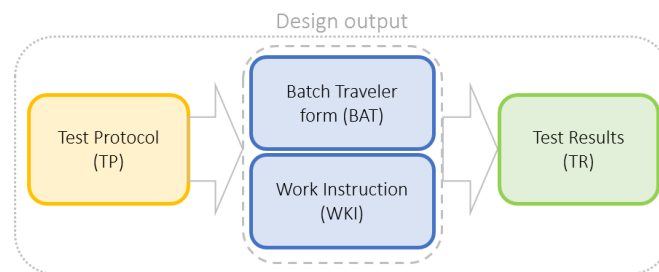


Figure 31 : Administrative forms trough which an operator has to conduct its experiment for an experiment as part of the Design output

The Test Protocol has to contain (i)a list of the materials and a description of the experimental procedure, (ii)references of Batch Traveler (BAT) and Work Instruction (WKI) used for the experiment, (iii)a detailed explanation and example of the expected outcomes of the experiment and (iv)the Test Result (TR) to-be reference.

The Batch Traveler aims to assist the operator (the person responsible of the experiment) to register steps of the experiment by making the operator fill the list of available materials, the reference of said material, the batch numbers of each devices, samples and tools used during the experiment.

The Work Instruction aims to detail each steps of the experiment that the operator has to conduct.

Finally the Test Results aim to present the results and bring a conclusion to the expected outcomes listed in the TP.

BAT and WKI are live documents, which means that they may be changed over time if a correction needs to be done, unlike TPs and TRs that, once prepared and filled, have to be verified and fixed as record. TR are therefore the conclusion to an experiment and aimed to be used as such.

Once the TP, BAT and WKI has been written the operator can conduct the test and conclude on it through the TR.

This procedure is necessary to keep track of the tests realized on the device, as one should be able to verify conclusions and results for potential improvements or modification of the device testing.

Importance of inclusion/exclusion criteria

The outcome of a test can be interpreted very differently depending on the inputs of the tests and how the results are interpreted. For instance, for the electromechanical characterization, one of the expected outcome is the yield of the device. This yield refers to the amount of working samples once fabricated compare to the total amount of fabricated samples. The yield characterize in that case the success of the whole fabrication process.

Therefore, are not taken into consideration the samples on which we have a doubt on the origin of the failure, as it could come from a mis-manipulation outside of the fabrication process. Hence, if another operator was to do the same test, she/he would have to know these inclusion/exclusion criteria.

Importance of pass/fail criteria

Experiments and tests are ran on devices to determine their functional limits towards their future application. However, without a proper definition of targeted values or expected results to obtain, the testing could be infinite. If we take the example of the bonding tests, we realized that the test we were conducting were interesting toward the knowledge we could gain on the silicone-silicone adhesion, but it was not focused on the future application of the device. Therefore, a new experiment has been designed, where the pass criteria is the verification of the hermeticity of the bonding, rather than a force applied. From a more general point-of-view, when testing a device that aim to be developed, the definition of a clear pass/fail criteria make the operator and the organization gain time as not further experiment needs to be ran if the device is tested properly.

3.2 ADJACENT TRACKS ELECTRICAL INSULATION

This chapter aims at demonstrating the implementation of such administrative procedure to the tests we were conducting on the aspects of the device, such as hermetic encapsulation or electromechanical characterization. Moreover, as explained before, we wanted to implement a test that would better mimic the conditions of use of the device. We have therefore written TPs and TRs that correspond to the various tests conducted. In addition, we have set up a new test, which is close to the use that is made of the system. This example is shown in the following chapter.

SOFT ECoGs aim to be used as subdural electrodes as intraoperative neuromonitoring or as pre-surgical epilepsy detection. We have seen that in the case of the monitoring of epileptic seizures, the device would require to be implanted for a period of 2 to 3 weeks. And, as we have seen through the aging tests realized in the bonding of silicone stacks, the fluids surrounding the sample have an effect on the bonding of the silicone stacks.

The hermetic encapsulation could therefore be compromised, potentially allowing leachable to be released in the patient's body but also deteriorating the functionality of the device. In fact, there could be some adjacent tracks electrical interferences appearing between the tracks.

Therefore the set-up aim to let fully functional samples soak in the PBS solution at 37°C, for 31 days, to mimic the environment in which the device would be embedded in one of its main situation of use.

3.2.1 Materials and method

The soaking samples are similar to the ones presented in Figure 20 and Figure 22. The disposition of the samples in the PBS solution is presented on Figure 32. The principle being to have the track dipped into the PBS solution while leaving the connector dry in order to estimate the crosstalk solely caused by liquid potentially reaching the bonding interface.

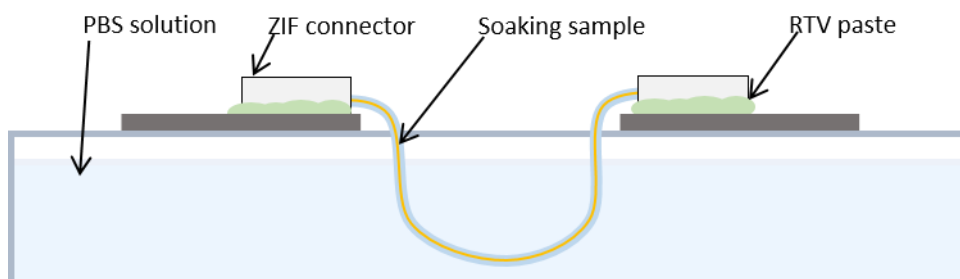


Figure 32 : Electrical insulation hermeticity experiment set-up

Through 31 days of soaking, for different time stamps, a current of maximum **1mA**, for a voltage of **2.1V**, is applied between the gold tracks, and the resistance is measured (the device used is a *Keithley 6430 Sub-femtoAmp Remote SourceMeter® RMU Instrument*). As stated by Shepherd et al. (2018) [28], “Crosstalk impedance approaching an order of magnitude more than the impedance of the electrodes are considered unacceptable.”. The initial resistance of the tracks are of the order of 10 kOhm, it is therefore considered that there is an **electrical leakage** if the resistance measured between the lines is of the order of **100 kOhms**. However we decided to set a **security limit to 1 MOhms**.

Two types of silicones were tested. The Silbione® M140 and Sylgard© 184. Six samples are made of Sylgard© 184 and seven are made of Silbione® M140, which make a total of 13 samples. For each samples there are 8 tracks, and therefore 7 inter-channel interference possibility per sample. Moreover inter-tracks are referred as inter-channel as well.

3.2.1.1 Exclusion criteria

All samples that may appear faulty, but for other reasons than a failure

1. In the fabrication process
2. in the hermetic encapsulation

are to be excluded from the measurements conducted during the experiments.

3.2.1.2 Pass/fail criteria

Outcome 1 : Electrical leakage

It is considered that there is an electrical leakage if the inter-channel impedance is of the order of 100 kOhm. Each sample presenting this characteristic will be considered faulty.

Outcome 2 : Delamination

It is considered that there is a failure in the hermetic encapsulation if, during the soaking period or during the electromechanical characterization, the silicone-silicone bonding appear to delaminate by itself.

3.2.2 Results and discussion

On the following graphs (Figure 33 and Figure 34) one can see the evolution of the inter-channel resistance through time (represented by the percentage of inter-channel in a resistance range).

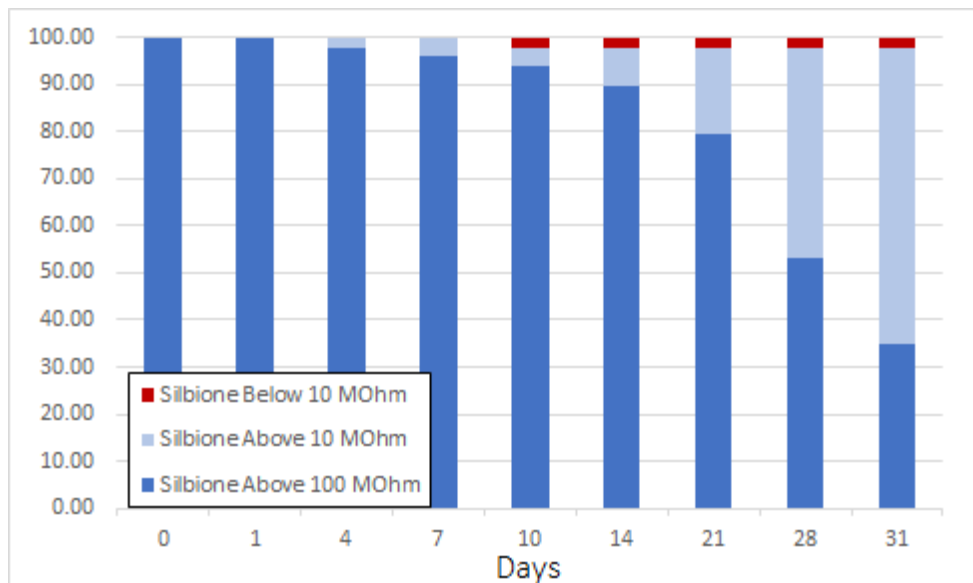


Figure 33 : Adjacent tracks current leakage tests on Silbione® M140 show an evolution of the inter-channel resistance through time

Sylgard 184© shows very similar results to the ones of Silbione® M140.

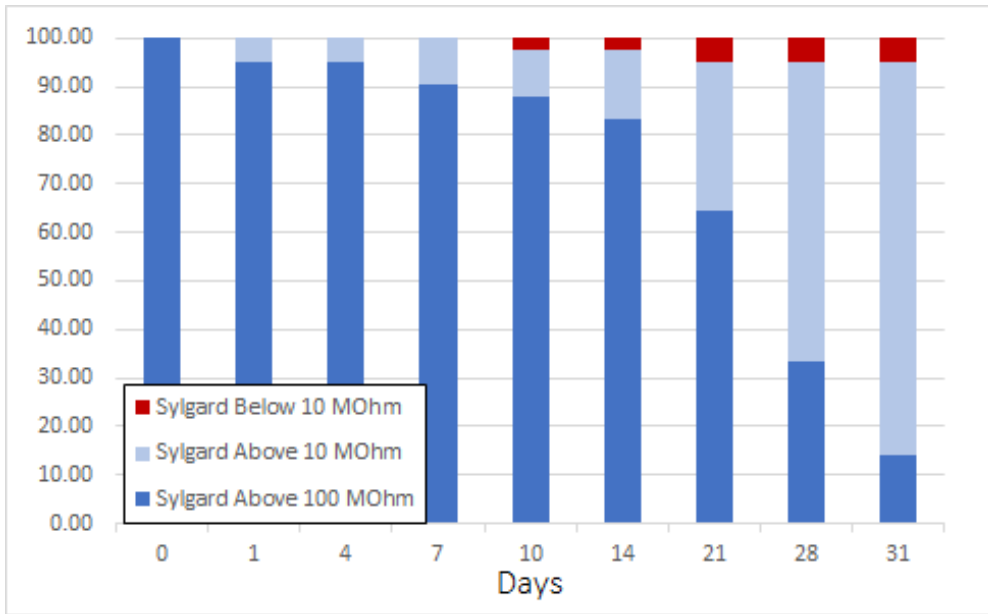


Figure 34 : Adjacent tracks current leakage tests on Sylgard 184© show an evolution of the inter-channel resistance through time

No impedance **below the magnitude of 1 MOhm** has been observed. For both material only a small percentage, not more than 5%, reach a current leakage that is considered as the limit. Therefore this experiment is conclusive on the insulation between tracks.

Following the measurement of the resistance through time during soaking, we wanted to observe the behavior of the samples during an electromechanical test. The resulting graph are on Figure 35. We have been able to plot only one sample for the Silbione® M140 as the test ended very recently.

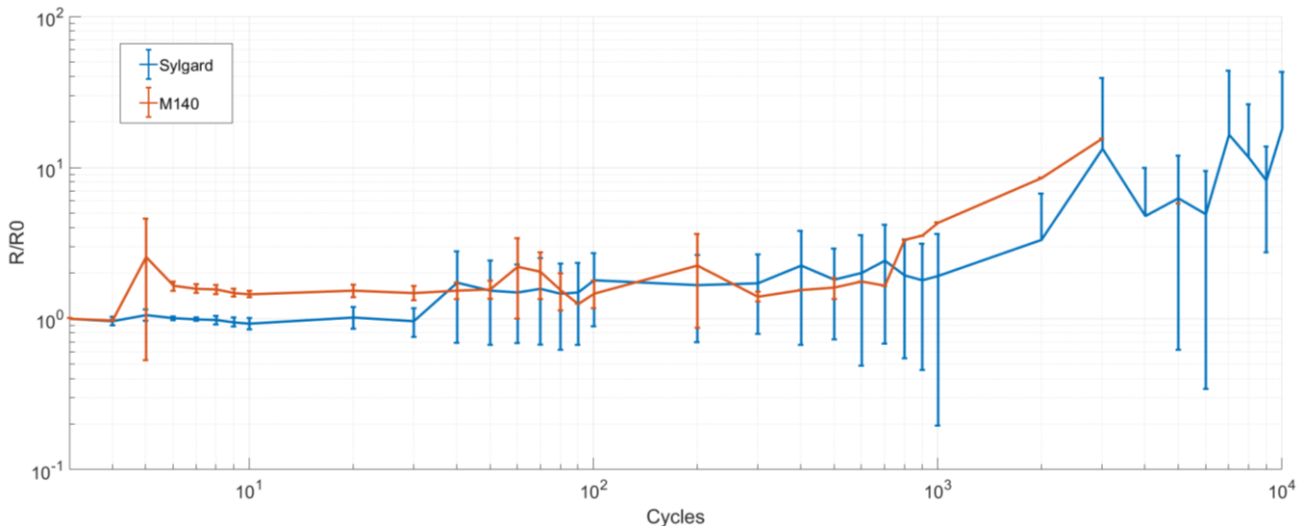


Figure 35 : Normalized impedance (avg+std) of the stretched samples after 31 days soaking in a PBS solution at 37°C, Sylgard 184© (blue, n=3) and Silbione® M140 (dark orange, n=1)

If we compare them to the curves on Figure 28 **Erreur ! Source du renvoi introuvable.**, these resistance evolution are rather high. However the samples never broke (mechanically speaking), and we think that some electrical failures were due to the deterioration of the ZIF connectors due to the manipulation during the experiment. For a first experiment of this kind it has therefore been a success.

The limitations of this experiment, with regard of the proximity with a real implantation, is the fact that no mechanical constraints are applied of the samples (movement of the brain inducing shear strength for example). An improved set-up would therefore reproduce the aging effect of the PBS solution, but would mirror the mechanical constraints present on a neural implant.

4 CONCLUSION

From the experiments and researches realized during this project the way is now paved for many improvements both regarding the testing of the device for clinical trial approval or for the research in many areas.

The bonding test showed promising results on the behavior of medical grade silicone (Silbione© M140) compared to an academic silicone (Sylgard 184©). The aging test demonstrate that there is an impact on both the mechanical characteristics of the silicone and on the bonding between stacks of silicone. It would however require more samples to be tested to determine a tendency in the aging. Similarly, the accelerated aging test showed that there is a possible correlation between the aging at 37°C and the aging at 37°C for an equivalent time, however because of the different type of failures after 1 week for the 37°C aging, it is not possible to draw any conclusion on this experiment. Finally the stiff-backing tests gave some promising results, but one would need to design something more reliable to test the adhesion energy.

These experiment also highlighted the fact that it is important to design in advance systematic testing method with a definition of the expected outcomes and inclusion/exclusion criteria, furthermore the need to make the link between the outcome of the test and how it is linked to the use of the device.

Finally the test of hermeticity of the silicone stacks bonding, ensuring as well the insulation of the tracks from each other, was successful, as no inter-channel resistance was measured below the limit we fixed of 1 MOhm.

In the continuity of the insulation test, another experiment could be designed in the same purpose, but including even more of the mechanical constraints present in the environment of an implanted subdural electrode, mimicking for example the pressure and shear strength that we find between the brain and the skull.

As for all the possible test that will be realized to verify the materials and method used for the fabrication of a clinical SOFT ECoG grid, each exclusion and pass/fail criteria shall be defined in a specifically designed protocol.

5 FUTURE PROSPECTS

During this project many paths of research has been open and studied. Even if they were not always relevant towards what we were aiming for with this project, they are subject of studies that could give other answers in the material research around SOFT ECoGs. Here are therefore presented some of these possible studies.

Considering the formation of microcracks in the gold layer, one could study the relation between gold and silicone, during the fabrication process (evaporation) and after the process (stretched silicone substrate). The study of **Coefficient of Thermal Expansion (CTE)** on cured silicone could give a hint on the behavior of the silicones during evaporation. In fact, the evaporation chamber shows a change in temperature during the evaporation, however the displacement of the silicones (both medical grade and academic grade) is not well known yet. Moreover, as stated by Zhao et al. (2019) when talking about thermal effects on the stretchable gold films, “[...]the thermal mismatch stress plays a key role in affecting the performance of the stretchable gold film electrodes whether in the electrical or thermal treatment process.” [31].

Another interesting path to follow would be a research on the potential **correlation between the density of microcracks and the electrical characteristics** of a gold layer. In their paper Zhao et al. (2019) make a link between the percentage of microcracks in a SEM image and the current density. It could therefore be possible to conclude on the possibility to determine the electrical characteristics of a gold track only through the visual analysis of the SEM image.

The formation of microcracks seem to depend on the deposition rate as well. Indeed, as showed by Matsuhisa et al. (2019) [32], for the same deposited Au (gold) thickness, the **resistance under strain changes depending on the deposition rate**.

During this project a major aspect that has been studied is the hermetic encapsulation, through the bonding of the silicone stacks. To observe the adhesion energy of such bonding, many types of tests exist through the literature. The **blister test**, as proposed by Lu et al. (2007) [21] could be set in place and tried, it however require a rather specific and bulky installation. The **pressure test** proposed by Eitner et al. (2014) [22] could also be implemented, but predictive model and a simulation model should be designed first (mathematical model and Comsol© simulation for instance).

6 REFERENCES

- [1] G. Schalk et E. C. Leuthardt, «Brain-Computer Interfaces Using Electrographic Signals,» *IEEE Reviews in Biomedical Engineering*, vol. 4, n° 110.1109, pp. 140-154, 2011.
- [2] J. N. Mak et J. R. Wolpaw, «Clinical Applications of Brain-Computer Interfaces : Current state and Future Prospects,» *IEEE Review of Biomedical Engineering*, vol. 1, n° 110.1109/RBME.2009.2035356, pp. 187-199, 2009.
- [3] N. Obidin, F. Tasmin et C. Dagdeviren, «The Future of Neuroimplantable devices : A Material Science and Regulatory Perspective,» *Advanced Material*, 12 April 2019.
- [4] O. Graudejus, P. Görrn et S. Wagner, «Controlling the Morphology of Gold Films on Poly(DiMethylSiloxane),» *Advanced Material and Interfaces*, pp. 1927-1933, 21 June 2010.
- [5] B. Zhu, S. Gong et W. Cheng, «Softening gold for elastronics,» *Royal Society of Chemistry*, pp. 1668-1711, 30 July 2014.
- [6] S. P. Lacour, G. Courtine et J. Guck, «Materials and technologies for soft implantable neuroprostheses,» *Springer Nature*, vol. 1, pp. 1-14, October 2016.
- [7] S. P. Lacour, D. Chan, S. Wagner, T. Li et Z. Suo, «Mechanisms of reversible stretchability of thin metal films on elastomeric substrates,» *Applied Physics Letters*, pp. 204103-1-3, 22 March 2006.
- [8] S. P. Lacour, S. Wagner et Z. H. a. Z. Suo, «Stretchable gold conductors on elastomeric substrates,» *Applied Physics Letters*, pp. 2404-2406, 13 February 2003.
- [9] B. R. A. Neves, J. M. C. Vilela, P. E. Russell, A. C. C. Reis et M. S. Andrade, «Imaging micro-cracks in gold films : a comparative study of scanning tunneling and atomic force microscopies,» *Elsevier*, pp. 61-67, 1999.
- [10] N. Bowden, W. T. S. Huck, K. E. Paul et G. M. Whitesides, «The controlled formation of ordered sinusoidal structures by plasma oxidation of an elastomeric polymer,» *Applied Physics Letters*, pp. 2557-2559, 01 September 1999.
- [11] N. Bowden, S. Brittain, A. G. Evans, J. W. Hutchinson et G. M. Whitesides, «Spontaneous formation of ordered structures in thin films of metals supported on an elastomeric polymer,» *Letters to Nature*, pp. 146-149, 14 May 1998.
- [12] O. Graudejus, Z. Yu, J. Jones, B. Morrison et S. Wagner, «Characterization of an elastically stretchable microelectrode array and its application to neural field potential recording,» *Journal of The Electrochemical Society*, pp. 85-94, 21 April 2009.
- [13] T. Adrega et S. P. Lacour, «Stretchable gold conductors embedded in PDMS and patterned photolithography : fabrication and electromechanical characterization,» *Journal of Microengineering*, pp. 1-8, 2 March 2010.
- [14] I. R. Mineev, P. Musienko, Q. B. A. Hirsch, E. M. M. N. Wenger, J. Gandar, M. Capagrosso, T. Milekovic, L. Asboth, R. F. Torres, N. Vachicouras, Q. Liu, N. Pavlova, S. Duis, A. Larmagnac, J.

- Vörös, S. Micera, Z. Suo et G. Courtine, «Electronic dura mater for chronic multimodal neural interfaces,» *Science*, pp. 1-64, 2015.
- [15] D. Campbell, K. J. Beckman, C. E. Calderon, P. W. Doolan, R. M. Ottosen, A. B. Ellis et G. C. Lisensky, «Replication and compression of bulk and surface structures with polydimethylsiloxane elastomer,» *Journal of Chemical Education*, pp. 537-541, 4 April 1999.
- [16] Elkem, «Silbione (R) BIOMEDICAL LSR M100 series - Liquid Silicone Rubber - Long-Term Implant,» October 2017. [En ligne]. Available: <http://www.silbione.com/wp-content/uploads/2017/11/Silbione-LSR-M1XX.pdf>. [Accès le April 2019].
- [17] NUSIL, «MED-4211 Low consistency silicone elastomer,» 26 November 2018. [En ligne]. Available: <https://nusil.com/services/downloadfile.ashx?productcode=MED-4211&originalname=MED-4211.pdf>. [Accès le Mai 2019].
- [18] J. Bourely, «Implementation of Medical Grade Materials in Soft Neural Implants for Clinical Use,» January, Geneva, 2019.
- [19] K. E. Herold et A. Rasooly, *Lab-on-a-chip Technology (Vol.1): Fabrication and Microfluidics*, Bethesda: Caister Academic Press, 2009.
- [20] S. Bhattacharya, A. Datta, J. M. Berg et S. Gangopadhyay, «Studies on surface wettability of Poly(dimethyl)siloxane (PDMS) and glass under oxygen-plasma treatment and correlation with bond strength,» *Journal of Microelectromechanical Systems*, pp. 590-597, June 2005.
- [21] Y.-W. Lu et P.-T. Lin, «A line force model to measure the strength of polydimethylsiloxane (PDMS)-to-PDMS bonding using blister tests,» *NSTI-Nanotech*, pp. 190-193, 2007.
- [22] U. Eitner et L. C. Rendler, «The mechanical theory behind the peel test,» *Elsevier*, pp. 331-335, 2014.
- [23] M. A. Eddings, M. A. Johnson et B. K. Gale, «Determining the optimal PDMS-PDMS bonding technique for microfluidic devices,» *Journal of Micromechanics and Microengineering*, pp. 1-4, 25 April 2008.
- [24] K. J. Hemmerich, «General aging theory and simplified protocol for accelerated aging of medical devices,» *Medical Device and Diagnostic Industry Journal*, July 1998. [En ligne]. Available: <https://www.mddionline.com/general-aging-theory-and-simplified-protocol-accelerated-aging-medical-devices>. [Accès le April 2019].
- [25] P. S. T. Limited(TM), «MED-4210P,» 22 June 2007. [En ligne]. Available: <https://www.silicone-polymers.co.uk/pdfMaster/MED-4210P.pdf>. [Accès le March 2019].
- [26] M. V. Hoang, H.-J. Chung et A. L. Elias, «Irreversible bonding of polyimide and polydimethylsiloxane (PDMS) on a thiol-epoxy click reaction,» *Journal of Micromechanics and Microengineering*, pp. 1-9, 19 September 2016.
- [27] N. Vachicouras, «Soft Microfabricated Neural Implants : A Path Towards Translational Implementation,» EPFL and Bertarelli Foundation, Genève, 2019.

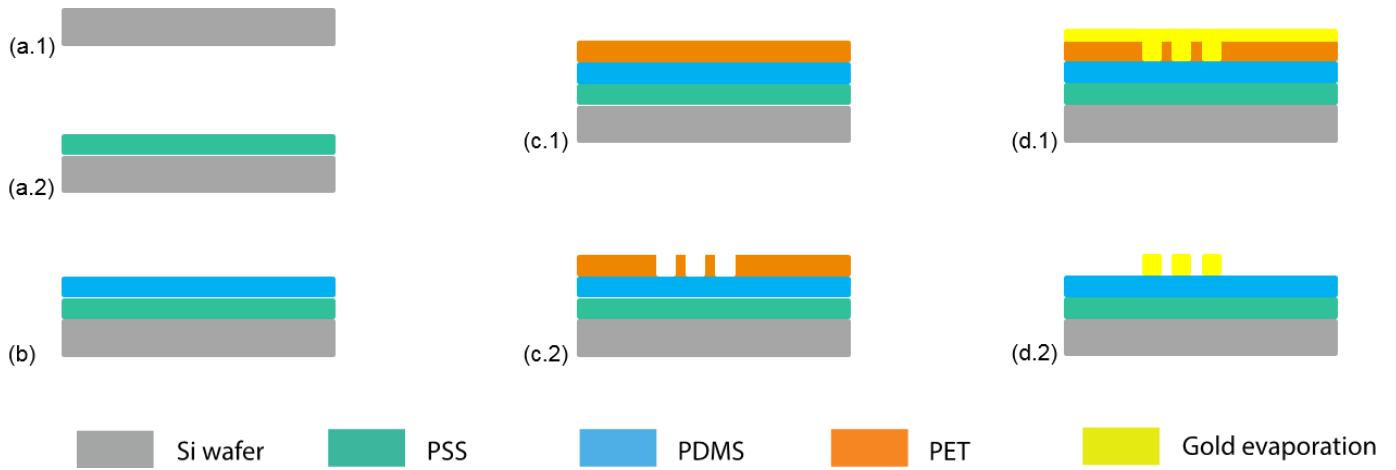
- [28] R. K. Shepherd, J. Villalobos, O. Burns et D. A. X. Nayagam, «The development of neural stimulators : a review of preclinical safety and efficacy studies,» *Journal of Neural Engineering*, pp. 384-388, 01 August 2018.
- [29] L. Ravagnan, G. Corbelli, C. Ghisleri, P. Milane et M. Marelli, «Method for the production of functionalized elastomeric manufacturer articles and manufactured articles thus obtained». United States Brevet US 2019/0203341 A1, 4 July 2019.
- [30] R. K. Shepherd, *The Biomedical Engineering of Neural Prostheses*, Melbourne: John Wiley & Sons, Inc., 2016.
- [31] Y. Zhao, M. Yu, Z. Liu et Z. Yu, «Electrical and thermal effects on electromechanical performance of stretchable thin gold films on PDMS substrates for stretchable electronics,» *Journal of Applied Physics*, pp. 165305-1-7, 28 March 2019.
- [32] N. Matsuhisa, Y. Jiang, Z. Liu, G. Chen, C. Wan, Y. Kim, J. Kang, H. Tran, H.-C. W, I. You, Z. Bao et X. Chen, «High-transconductance stretchable transistors Achieved by controlled Gold microcrack morphology,» *Advanced Electronic Materials*, pp. 1-10, 6 June 2019.

7 ANNEXES

A1 – Definitions

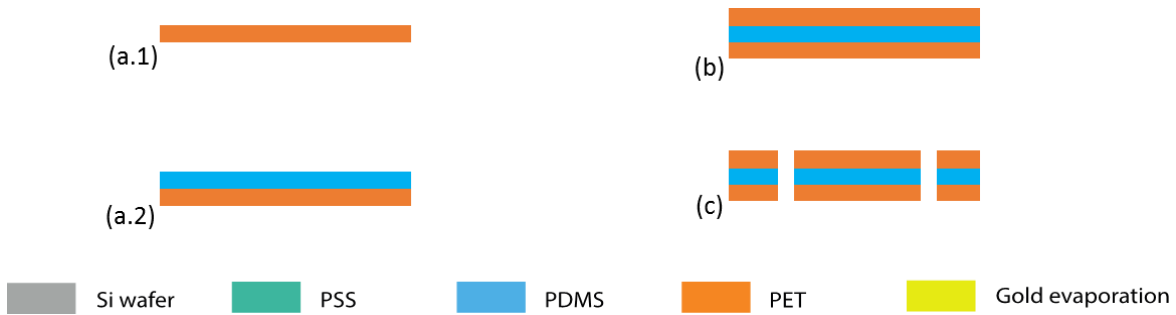
CNS	Central Nervous System
PNS	Peripheral Nervous System
MEAs	MicroElectrode Arrays
EEG, ECoG, AP/LFP	ElectroEncephaloGram, ElectroCorticoGram, Action Potential/Local Field Potential
MRI	Magnetic Resonance Imaging
Silicone/PDMS	Poly(DiMethyl)Siloxane, which is addressed as silicone in the report
MDR	Medical Device Regulation
QMS	Quality Management Systems
EMA	European Medicines Agency
FDA	Food and Drug Administration
RTV	Room Temperature Vulcanize
PET	Poly (Ethylene Terephthalate)
LSR, HCR	Liquid Silicone Rubber, High Consistency Rubber
CE	Conformité Européenne
ZIF	Zero-Induced Force

A2 - Evaporation fabrication process



(a.1-2)	Wafer cleaning with IPA and N ₂ PSS spincoating (2000rpm)	(c.1)	PET sheet deposition	(d.1)	Chromium and Gold evaporation (5nm at 3.1A/s, 35nm at 5A/s)
(b)	Silicone spincoating (~340rpm)/blade coating (~1mm/s)	(c.2)	PET sheet laser cut (laser)	(d.2)	PET sheet peel-off

A3 – Encapsulation fabrication process



(a.1-2)	PET cleaning and installation Silicone spincoating (~340rpm)/blade coating (~1mm/s)	(c)	Encapsulation laser cut
(b)	Silicone encapsulation with cleaned PET sheet (23μm thick)		

A3 – Normalized resistance graphs for each samples of each materials

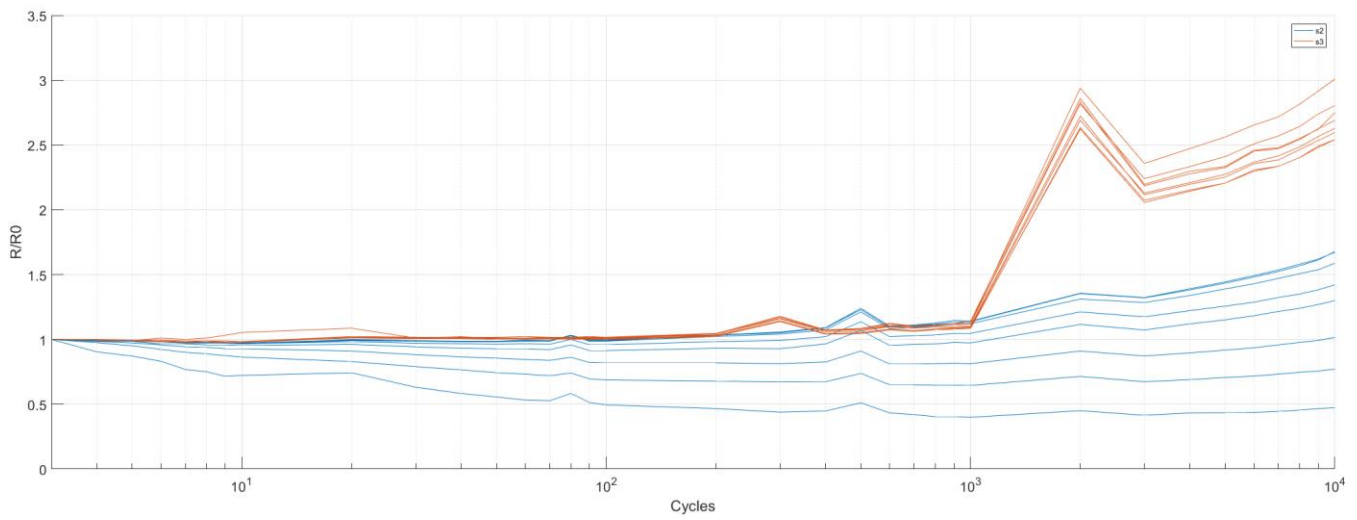


Figure 36 : Silbione M140 stretching cycles all separated

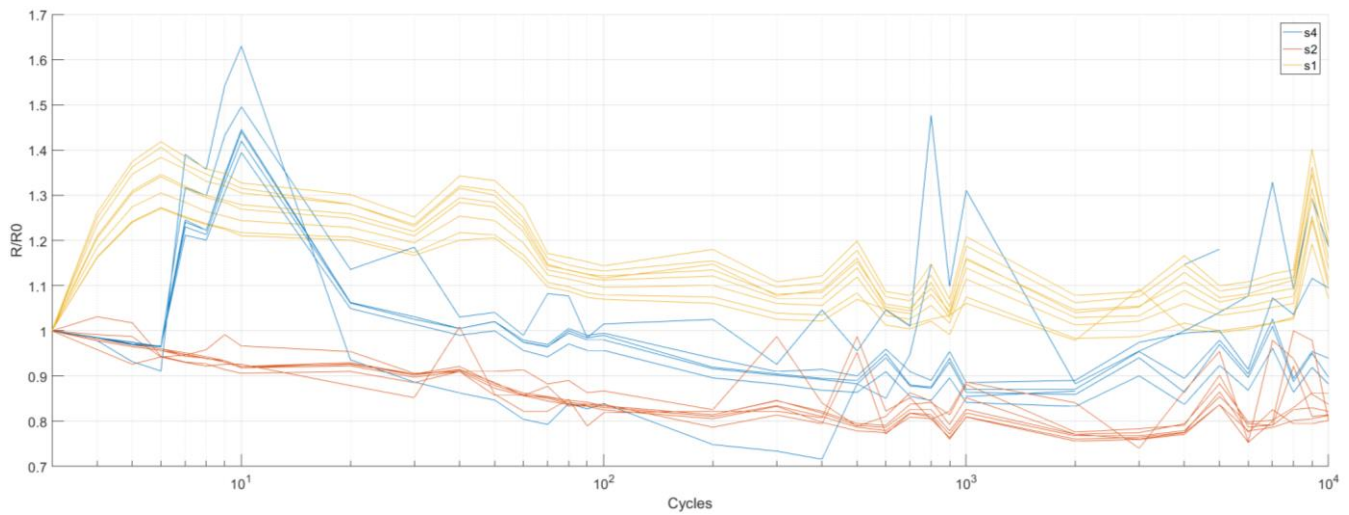


Figure 37 : Nusil™ MED-4211 stretching cycles all separated

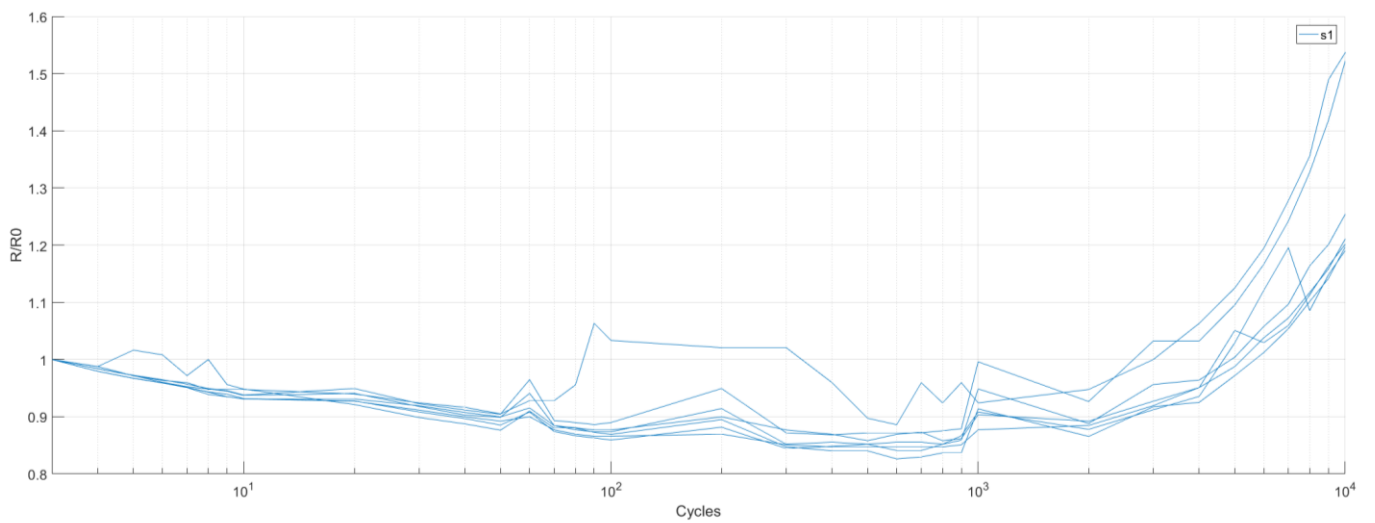


Figure 38 : Nusil™ MED-4210 stretching cycles all separated

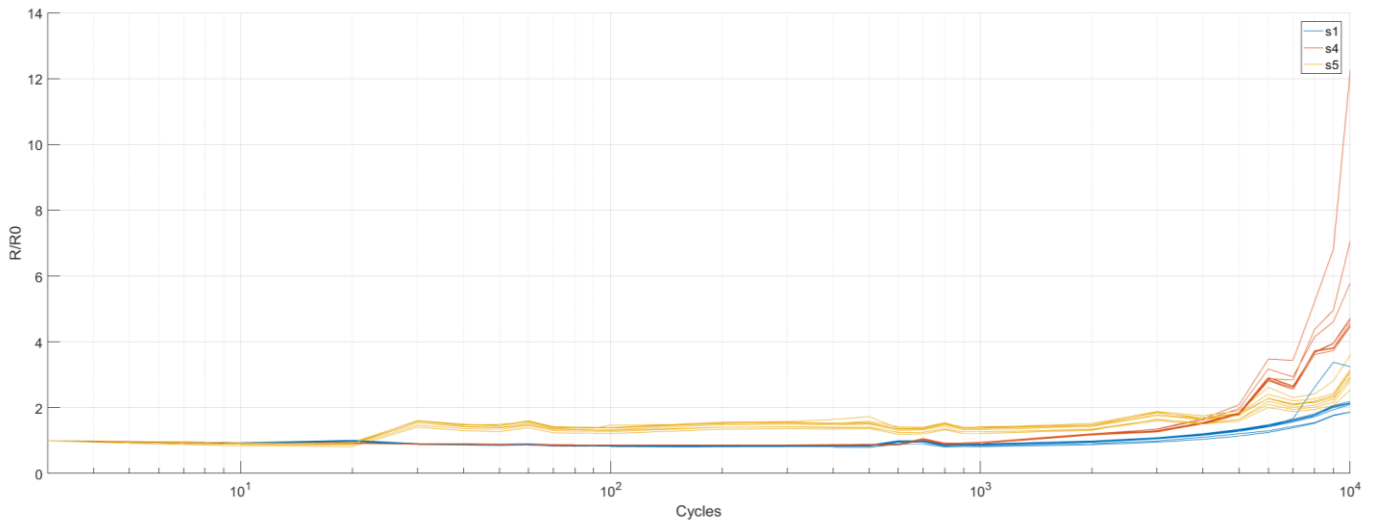


Figure 39 : Silbione® M130 stretching cycles all seperated

A4 - Costs analysis :

Cleanroom facilities	5'000.- chf
50 wafers	600.- chf
Gold (evaporation)	120.- chf
Laboratory facilities	200.- chf
Silbione© M140	3'000.- chf (~10'000.- chf for 3kg)
Total costs	8'920chf (~8'192.40 euros)